Iptycene-Containing Azaacenes with Tunable Luminescence

Iptycene Containing Azaacenes with Tunable Luminescence

Iptycene Containing Azaacenes with Tunable Luminescence

Journal:	*SYNLETT*
Manuscript ID	ST-2017-04-0234-L.R1
Manuscript Type:	Letter
Date Submitted by the Author:	n/a
Complete List of Authors:	Schleper, Lennart; MIT, Chemistry Voll, Constantin-Christian ; MIT, Chemistry Engelhart, Jens; MIT, Chemistry Swager, Timothy; MIT, Chemistry
Keywords:	arene, fluorescence, Nazarene, triptycene, charge transfer
Abstract:	An optimized route toward iptycene-capped, p-dibromo-quinoxalinophenazine 7 was developed, increasing the yield significantly from literature procedures. New iptycene containing symmetrical azaacenes were synthesized from this intermediate using Suzuki-Miyaura cross-coupling and their photophysical properties were evaluated. Tuning the substituents allows modulating emission wavelengths across the visible spectrum. Substitution with 3-methoxy-2-methylthiophene (12) exhibits a quantum yield of 35%. The (triisopropylsilyl)acetylene product 15 has a quantum yield of 38% and serves as a model compound for the synthesis of polymers based on this electrooptically-active molecular motif.

Iptycene Containing Azaacenes with Tunable Luminescence

A. Lennart Schleper[§]
Constantin-Christian A. Voll[§]
Jens U. Engelhart
Timothy M. Swager*

Department of Chemistry, Massachusetts Institute of Technology, 77 Massachusetts Avenue, Cambridge MA, 02139, USA
tswager@mit.edu

[§] These authors contributed equally

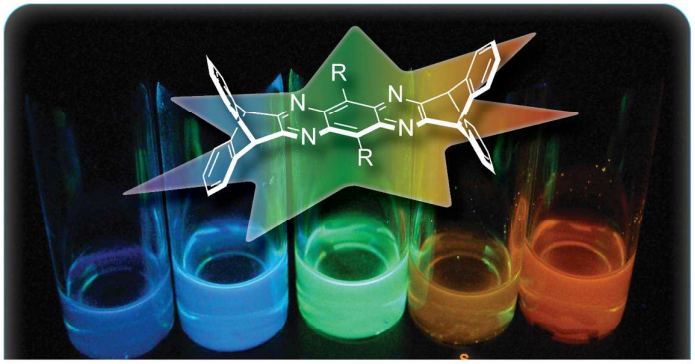

Received:
Accepted:
Published online:
DOI:

Abstract An optimized route toward iptycene-capped, *p*-dibromo-quinoxalinophenazine **7** was developed, increasing the yield significantly from literature procedures. New iptycene containing symmetrical azaacenes were synthesized from this intermediate using Suzuki-Miyaura cross-coupling and their photophysical properties were evaluated. Tuning the substituents allows modulating emission wavelengths across the visible spectrum. Substitution with 3-methoxy-2-methylthiophene (**12**) exhibits a quantum yield of 35%. The (triisopropylsilyl)acetylene product **15** has a quantum yield of 38% and serves as a model compound for the synthesis of polymers based on this electrooptically-active molecular motif.

Key words N-heteroiptycene, Suzuki-Miyaura cross-coupling, Sonogashira coupling, pyrazinoquinoxaline, luminescence

In recent years, there has been an immense interest in organic materials for OLEDs, OFETs and PVs, encouraged by the ease of tunability through design and solubility compared to inorganic counterparts, which is conducive to large-scale printing techniques.[1,2] OLEDs, as an example, initially struggled with efficiency because upon electrochemical excitation, singlet and triplet excitons are formed in a 1:3 statistical ratio.[3] Since only the radiative decay from singlet excitons is quantum chemically fully allowed and the long-lived triplet excitons usually relax through non-radiative processes, internal electroluminescent quantum efficiency (η_{int}) of most organics is limited to 25%. Phosphorescent materials and delayed fluorescence have been investigated as triplet harvesting strategies. Most of these materials incorporate heavy metals and have been shown to achieve η_{int} values that are essentially 100%. However, their use is constrained by cost, the limited stability of blue emitters, and triplet-triplet annihilation at high current densities.[4–6] Emissive stable radicals have also been considered, but there are currently only a limited number of structures suitable for this purpose and quantum efficiencies have thus far been low.[7,8] Recently high emission efficiencies from thermally activated delayed fluorescence (TADF) have been reported and this method is emerging as a promising approach to create efficient OLEDs.[9] Indeed this method tends to outperform the up-conversion of triplets to singlet excitons by triplet-triplet annihilation.[10–12] TADF requires the energetic proximity of the S_1 and T_1 state and the first-order mixing coefficients between singlet and triplet states are inversely proportional to the singlet-triplet gap (ΔE_{ST}).[13] This small ΔE_{ST} allows fast intersystem crossing for the thermal equilibration of triplet and singlet excitons. Electroluminescence with η_{int} approaching 100% have been realized through TADF.[9,14] There are two classes of TADF materials that meet the electronic requirements of a low ΔE_{ST}. A torsion angle between donor and acceptor moieties[9,15,16] or having the donor-acceptor groups in homoconjugation, both provide mechanisms to produce segregated HOMO and LUMO states that lower the exchange energy and give rise the small energy difference.[17] In fact, another promising approach for OLEDs and other optical applications involves the spatial segregation of FMOs. In this context we were interested in investigating cruciforms comprising two perpendicular π–conjugated linear units connected by a central aromatic core and thereby can reduce HOMO and LUMO orbital overlap.[18–22]

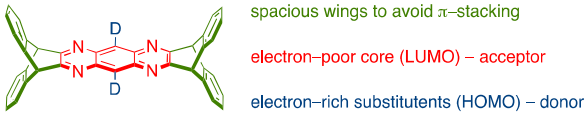

Figure 1: Generic target structures targeted in this publication.

We postulated the generic structure shown in Figure 1 to display favorable optical properties. The electron-deficient pyrazinoquinoxaline core will have little HOMO-LUMO orbital overlap with a relatively bulky electron donor that is forced to adopt a twisted conformation.[23,24] The three-dimensional structurally rigid iptycene wings minimize the typical tendency of azaacenes for π-stacking that can lead to self-quenching and reduced quantum yields.[25,26] The isolated phenyl groups of the iptycene wings are not expected to contribute significantly to the HOMO or LUMO.[27]

We targeted a modular synthetic route for symmetric azaacenes and envisioned **7** as a valuable key intermediate because the lateral aryl bromides allow functionalization through cross-coupling reactions. The diketone intermediate **4** was synthesized as shown in Scheme 1, through adaptation of a literature procedure that involves Diels-Alder reaction of anthracene with vinylene carbonate, followed by a basic hydrolysis and a Swern oxidation.[28]

Scheme 1. Synthetic procedure for the synthesis of intermediate **7**.

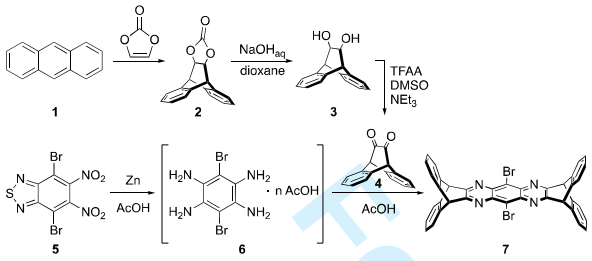

The condensation of **4** was complicated by the fact that 3,6-dibromobenzene-1,2,4,5-tetraamine (**6**) is unstable and has to be prepared *in situ*. Literature procedures for the reduction of 4,7-dibromo-5,6-dinitrobenzo[*c*][1,2,5]thiadiazole (**5**) followed by condensation to a diketone are generally low yielding (20 and 47% for related structures),[29,30] and as a result we decided to optimize the reaction cascade. Following the established literature procedure provided **7** in 33% yield (Entry 2, Table 1). Other reaction conditions such as varying the temperature, zinc-activation by hydrochloric acid, increasing the amount of zinc or the use of hydrochloric acid, instead of acetic acid, did not increase the yield of the reaction (Entries 1, 3 – 6, Table 1). Analysis of the reaction mixture revealed a considerable amount of residual diketone **4**, thus encouraging the use of an excess of **5**. Yields improved up to 65% when 1.38 equivalents of **5** were utilized (Entry 8, Table 1).

Table 1: Reaction optimization for the synthesis of **7**

Entry	T (°C)[a]	Activated Zinc[b]	Acid	Zinc (equiv.)	**5** (equiv.)	Yield (%)
1	50	No	AcOH	20	0.50	trace
2	60	No	AcOH	20	0.50	33[c]
3	70	No	AcOH	20	0.50	trace
4	60	Yes	AcOH	20	0.50	trace
5	60	No	HCl	20	0.50	trace
6	60	No	AcOH	200	0.50	trace
7	60	No	AcOH	20	1.25	61[c]
8	60	No	AcOH	20	1.38	65[c]
9	60	No	AcOH	20	1.50	57[c]
10	60	No	AcOH	20	1.38	72[c]

[a] Temperature used for reduction of **5** to **6** [b] Zinc activation by HCl [c] isolated yield

Having the tetraamine **6** in excess, however, increases the likelihood of mono-condensation hence the order of addition was reversed. Slowly adding the amine to a solution of the diketone in acetic acid over 1 h furthermore raised the yield to 72% (Entry 10, Table 1). Despite the promising increase in yield, we encountered issues in scaling up the reaction and diminished yields were observed at scales more than 60 mg of **4**.

Having optimized the first reaction cascade, we endeavored to introduce donor groups to **7** through cross-coupling reactions. We surveyed both Stille and Suzuki-Miyaura couplings, and converged on the latter based upon higher yields whilst avoiding toxic tin reagents. Reaction optimization with (3,5-dimethoxyphenyl)boronic acid revealed that cross-coupling to **7** could be achieved in 99% yield using $Pd_2(dba)_3$/P(*o*-tol)$_3$ as the catalyst at 60 °C. Other catalysts such as $Pd(PPh_3)_4$, the addition of CuI, Pd-XPhos-G2 or $Pd(dppf)Cl_2$ resulted in low to moderate yields (Table 2).

Table 2: Optimization of Suzuki-Miyaura cross-coupling

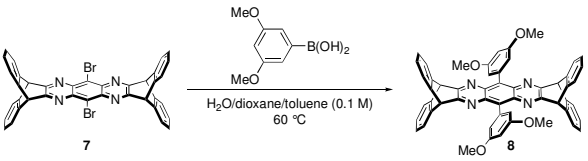

7 **8**

Entry	Catalyst	CuI (equiv.)	Yield (%)
1	$Pd(PPh_3)_4$	—	trace
2	$Pd(PPh_3)_4$	0.2	trace
3	Pd-XPhos-G2	—	47[a]
4	$Pd(dppf)Cl_2$	—	54[a]
5	$Pd_2(dba)_3$/P(*o*-tol)$_3$	—	99[a]

[a] isolated yield

The optimized reaction conditions were applied to a variety of (hetero)aryl boronic acids and the C-C cross-coupling products **9** – **13** could be obtained in yields ranging from 65 to 99% (Figure 2).

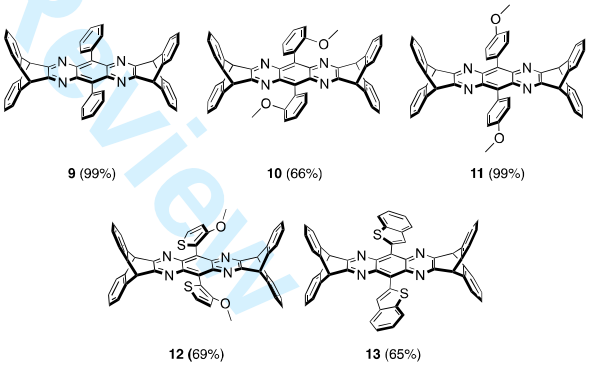

Figure 2: Substrate scope of aryl boronic acid coupling with **7**.

We furthermore attempted to extend the scope to include Pd-catalyzed *N*-arylation with carbazole in order to introduce stronger donors. Unfortunately, initial attempts using a variety of ligands (XPhos, *t*BuBrettPhos, RuPhos or *t*BuXPhos) only produced unreacted and reduced forms of **7**. However, the *N*-arylation with iminodibenzyl, which is known to be a better nucleophile than carbazole,[31] proceeded smoothly to give **14** in 56% yield using the Buchwald precatalyst Pd-RuPhos-G4 (Scheme 2).

Scheme 2. *N*-arylation reaction of iminodibenzyl with **7**.

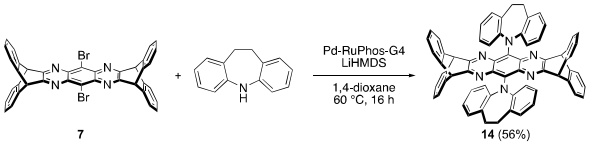

7 **14** (56%)

These promising coupling results with aryl bromides also encouraged us to synthesize a (triisopropylsilyl)acetylene product (**15**) via a Sonogashira reaction catalyzed by $Pd(PPh_3)_4$ and CuI in 57% yield (Scheme 3). This compound serves as a model compound for a hypothetical acetylene-linked polymer of **7**. The yield of the Sonogashira reaction in this case is too low to be of utility for the synthesis of polymers, which require near quantitative yields. We note that **15** has very recently been synthesized by Bunz and co-workers through a different synthetic route.[32]

Scheme 3: Sonogashira coupling of **7** with (triisopropylsilyl)acetylene to form **15**.

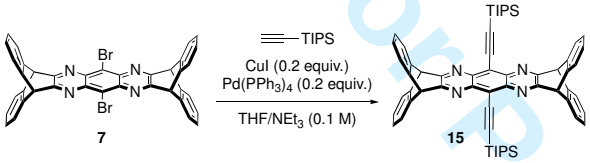

7 **15**

Photophysical Characterization

We were interested to determine if these materials displayed desirable optical properties, including TADF. Representative absorption spectra of the compounds **9-13** are shown in Figure 3. All of the compounds display vibronic fine structure with peaks that are summarized in Table 3. The broad tails at longer wavelength are suggestive of charge transfer character.

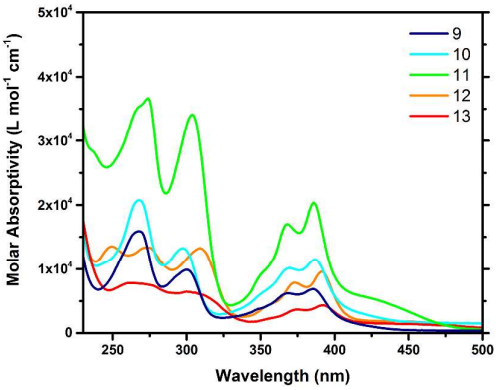

Figure 3: Absorption spectra with molar absorptivity for **9 – 13** in hexane.

To determine if this class of compounds display TADF behavior, we measured the quantum yields in both deoxygenated and oxygen-containing solvents. In TADF systems, triplet states contribute to a delayed component, which renders the compounds susceptible to quenching by oxygen.[33,34] An increase in quantum yield in an oxygen-free solvent is therefore an indication of TADF. As shown in Figure 4, compounds **9-13** were emissive, however saturating the solutions with oxygen did not significantly affect the quantum yield, thereby suggesting that these compounds are not TADF active or have a sufficient lifetime because of rapid non-radiative processes.

Compound **14**, which has a stronger donor in the iminodibenzyl group, was only weakly emissive as a result of a weak charge transfer band (Figure S10). Nevertheless, the absorption and emission compounds produced impressively cover essentially

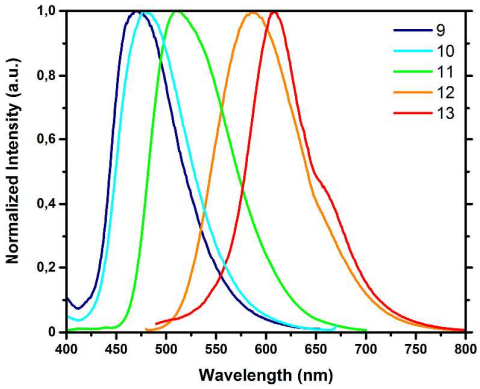

the whole visible spectrum.

Figure 4: Emission spectra of compounds **9 – 13** in hexane.

Table 3: Optical properties of compound **9 – 15**, measured in hexane.

Compound	λ_{max} (emis)	QY (%)	λ_{max} (abs)
9	470	2.2 x 10^{-3}	268, 300, 367, 385
10	478	0.06	268, 397, 368, 387
11	510	0.07	274, 303, 368, 386
12	586	0.35	248, 274, 309, 373, 397
13	608	0.11	266, 301, 374, 393
14	—	—	265, 360, 378, 400, 522
15	466, 495	0.29 (0.38)[a]	275, 307, 378, 400, 427, 454

[a] degassed by bubbling argon through solution

The (Triisopropylsilyl)acetylene product **15** shows several well-defined absorption maxima as shown in Figure 5. The compound is emissive with a maximum at 466 nm with a pronounced shoulder peak at 495 nm, to give a visibly green emission. The quantum yield was 38% in degassed hexane but decreased to 29% after oxygen exposure. This suggests the presence of long lived excited states, most likely triplet states, that are quenched by O_2.

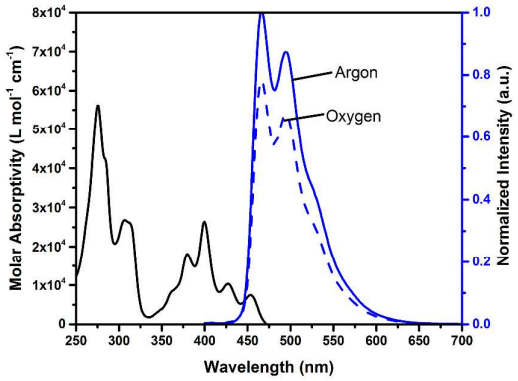

Figure 5: Photophysical characterization of **15**, measured in hexane.

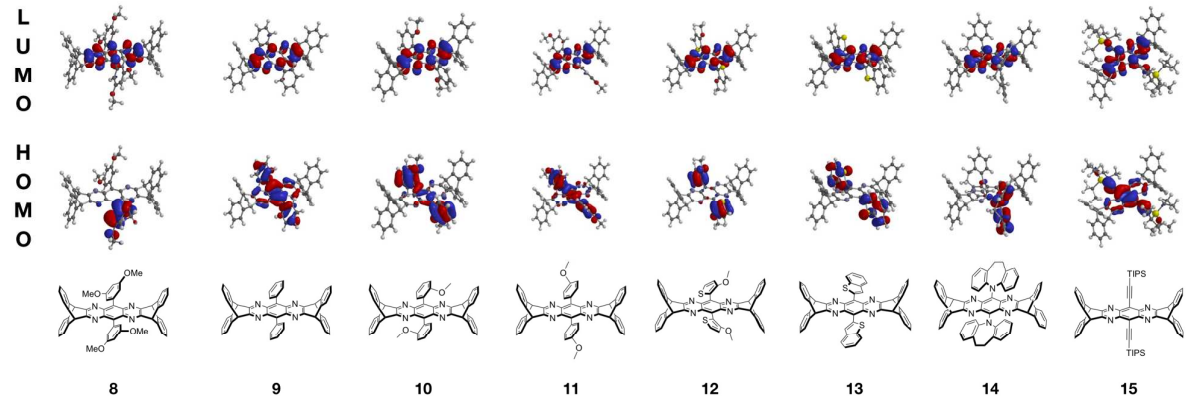

Figure 6: DFT calculations of HOMO and LUMO for compounds **8 – 15**. The calculations were performed using the B3LYP functional and 6-31+G* basis set.

We performed DFT calculations using the B3LYP functional and 6-31+G* basis set to evaluate the HOMO-LUMO separation of all of the products (Figure 6). They show, as anticipated, the iptycene wings do not contribute to either HOMO or LUMO states. The HOMO and LUMO frontier orbitals, however have sizable overlap in products **9**, **10** and **11**. The exchange energy that stabilizes the triplet is therefore significant and produces a larger ΔE_{ST} that decreases the coupling between the singlet and triplet states and reduces RISC. This is consistent with the experimental data that the aryl substituted products are TADF inactive. Our DFT calculations suggest that products **8**, **12** and **13** seem to have favorable spatial HOMO-LUMO separation that provides only minor orbital overlay and at the onset we expected these compounds to be TADF active. However, these are gas phase, ground state, calculations with equilibrium conformations. It is possible that in the excited state conformations and dynamics are present that promote larger ΔE_{ST} and competitive nonradiative relaxations. With regard to the latter, the quantum yields of these materials are modest to low. The TIPS-acetylene product **15** shows high overlap between the HOMO and LUMO states. This is inconsistent with TADF behavior. This effect may be the result of the silicon groups, however conformation of the origin of the intersystem crossing will require additional investigations that are beyond our initial synthetic studies that are the focus of this publication.

In conclusion, we report the synthesis of **7** through an optimized synthetic route. The in situ reduction of 4,7-dibromo-5,6-dinitrobenzo[*c*][1,2,5]thiadiazole was optimized to boost the yield to 72%. The versatility of the dibromoaryl intermediate **7** was exemplified in a variety of Suzuki-Miyaura cross-coupling reactions that proceed in moderate to excellent yields (65 – 99%), a Pd-catalyzed *N*-arylation with iminodibenzyl, and a Sonogashira reaction with (triisopropylsilyl)acetylene. Most of the products are luminescent with emission colors ranging from blue to orange. We anticipate this molecular scaffold could potentially be used to create new materials with useful electrooptical properties.

Acknowledgment

Financial support was provided through the Airforce Office of Scientific Research, a Cusanuswerk scholarship of ALS, a MITei fellowship of CCAV sponsored by Eni S.p.A., and the German Research Foundation (DFG) of JUE.

Supporting Information

Yes

Primary Data

No

References and Notes

(1) Krebs, F. C. *Sol. Energy Mater. Sol. Cells* **2009**, *93* (4), 394–412.
(2) Burgues-Ceballos, I.; Stella, M.; Lacharmoise, P.; Martinez-Ferrero, E. *J. Mater. Chem. A* **2014**, *2* (42), 17711–17722.
(3) Segal, M.; Baldo, M.; Holmes, R.; Forrest, S.; Soos, Z. *Phys. Rev. B* **2003**, *68* (7), 1–14.
(4) Adachi, C.; Baldo, M. A.; Thompson, M. E.; Forrest, S. R. *J. Appl. Phys.* **2001**, 90 (10), 5048–5051.
(5) Hashimoto, M.; Igawa, S.; Yashima, M.; Kawata, I.; Hoshino, M.; Osawa, M. *J. Am. Chem. Soc.* **2011**, 133 (27), 10348–10351.
(6) Baldo, M. A.; Adachi, C.; Forrest, S. R. *Phys. Rev. B - Condens. Matter Mater. Phys.* **2000**, 62 (16), 10967–10977.
(7) Peng, Q.; Obolda, A.; Zhang, M.; Li, F. *Angew. Chemie - Int. Ed.* **2015**, 54 (24), 7091–7095.
(8) Obolda, A.; Ai, X.; Zhang, M.; Li, F. *ACS Appl. Mater. Interfaces* **2016**, 8, 35472–35478.
(9) Uoyama, H.; Goushi, K.; Shizu, K.; Nomura, H.; Adachi, C. *Nature* **2012**, 492 (7428), 234–238.
(10) Luo, Y.; Aziz, H. *Adv. Funct. Mater.* **2010**, 20 (8), 1285–1293.
(11) Kondakov, D. Y.; Pawlik, T. D.; Hatwar, T. K.; Spindler, J. P. *J. Appl. Phys.* **2009**, 106 (12), 124510.
(12) Li, W.; Pan, Y.; Xiao, R.; Peng, Q.; Zhang, S.; Ma, D.; Li, F.; Shen, F.; Wang, Y.; Yang, B.; Ma, Y. *Adv. Funct. Mater.* **2014**, 24 (11), 1609–1614.
(13) Cui, L.-S.; Nomura, H.; Geng, Y.; Kim, J. U.; Nakanotani, H.; Adachi, C. *Angew. Chemie Int. Ed.* **2017**, 56, 1571–1575.
(14) Turro, N. J. Modern Molecular Photophysics; Benjamin Cummings, **1978**.
(15) Nakanotani, H.; Higuchi, T.; Furukawa, T.; Masui, K.; Morimoto, K.; Numata, M.; Tanaka, H.; Sagara, Y.; Yasuda, T.; Adachi, C. *Nat. Commun.* **2014**, 5, 4016.
(16) Goushi, K.; Yoshida, K.; Sato, K.; Adachi, C. *Nat. Photonics* **2012**, 6 (4), 253–258.
(17) Kawasumi, K.; Wu, T.; Zhu, T.; Chae, H. S.; Van Voorhis, T.; Baldo, M. A.; Swager, T. M. *J. Am. Chem. Soc.* **2015**, 137 (37), 11908–11911.
(18) Chavez III, R.; Cai, M.; Tlach, B.; Wheeler, D. L.; Kaudal, R.; Tsyrenova, A.; Tomlinson, A. L.; Shinar, R.; Shinar, J.; Jeffries-EL, M. *J. Mater. Chem. C* **2016**, *4* (17), 3765–3773.
(19) Lim, J.; Albright, T. A.; Martin, B. R.; Miljanić, O. S. *J. Org. Chem.* **2011**, *76* (24), 10207–10219.
(20) Marsden, J. A; Miller, J. J.; Shirtcliff, L. D.; Haley, M. M. *J. Am. Chem. Soc.* **2005**, *127*, 2464–2476.
(21) Zucchero, A. J.; McGrier, P. L.; Bunz, U. H. F. *Acc. Chem. Res.* **2010**, *43*, 397–408.
(22) Kivala, M.; Diederich, F. *Acc. Chem. Res.* **2009**, *42*, 235–248.
(23) Endo, A.; Sato, K.; Yoshimura, K.; Kai, T.; Kawada, A.; Miyazaki, H.; Adachi, C. *Appl. Phys. Lett.* **2011**, 98 (8), 10–13.

(24) Hirata, S.; Sakai, Y.; Masui, K.; Tanaka, H.; Lee, S. Y.; Nomura, H.; Nakamura, N.; Yasumatsu, M.; Nakanotani, H.; Zhang, Q.; Shizu, K.; Miyazaki, H.; Adachi, C. *Nat. Mater*. **2015**, 14 (3), 330–336.
(25) Anthony, J. E. *Chem. Rev*. **2006**, 106 (12), 5028–5048.
(26) Li, J.; Zhang, Q. *ACS Appl. Mater. Interfaces* **2015**, 7 (51), 28049–28062.
(27) Swager, T. M. *Acc. Chem. Res.* **2008**, 41 (9), 1181–1189.
(28) Wright, M. W.; Welker, M. E. *J. Org. Chem*. **1996**, 61, 133–141.
(29) Zhang, L.; Jiang, K.; Li, G.; Zhang, Q.; Yang, L. *J. Mater. Chem. A* **2014**, 2, 14852–14857.
(30) Wang, E.; Hou, L.; Wang, Z.; Hellström, S.; Mammo, W.; Zhang, F.; Inganäs, O.; Andersson, M. R. *Org. Lett*. **2010**, 12 (20), 4470–4473.
(31) Huang, W.; Buchwald, S. L. *Chem. - A Eur. J*. **2016**, 22, 14186–14189.
(32) Ganschow, M.; Koser, S.; Hahn, S.; Rominger, F.; Freudenberg, J.; Bunz, U. H. F. *Chem. - A Eur. J.* **2017**, 23, 4415-4421.
(33) Tao, Y.; Yuan, K.; Chen, T.; Xu, P.; Li, H.; Chen, R.; Zheng, C.; Zhang, L.; Huang, W. *Adv. Mater.* **2014,** *26* (47), 7931-7958.
(34) Zhang, Q.; Li, J.; Shizu, K.; Huang, S.; Hirata, S.; Miyazaki, H.; Adachi, C. *J. Am. Chem. Soc.* **2012,** *134* (36), 14706-14709.
(35) Preparation of **2** and **3**
Following a literature procedure[21]
(36) Preparation of **7**
The optimized reaction was carried out in a 20 mL vial, containing zinc powder (470 mg, 7.19 mmol) suspended in AcOH (3.5 mL). Under stirring **5** (138 mg, 358 µmol) was added and the reaction mixture was heated to 60 °C for 1 h. The reduced colorless intermediate **6** was separated from the zinc powder by filtration through a pad of celite and added dropwise to a solution of **4** (61 mg, 260 µmol) in AcOH (1.5 mL) over 1 h. A yellow precipitate immediately formed. The solution was stirred for another 1 h and extracted several times with CH_2Cl_2 (20 mL) until the organic phase was colorless. The combined organic layers were washed with an aqueous $NaHCO_3$ solution (100 mL) and water (100mL). After evaporation of the solvent, the crude product was purified via column chromatography (SiO_2, hexane/CH_2Cl_2 3:1 → 0:1). The product (**7**, 65 mg, 93.8 µmol, 72%) was obtained as a yellow powder. ^{1}H-NMR (400 MHz, $CDCl_3$) δ [ppm] = 7.59 (dd, *J3* = 5.4 Hz, *J4* = 3.2 Hz, 4H, CH), 7.17 (dd, *J3* = 5.4 Hz, *J4* = 3.2 Hz, 4H, CH), 5.84 (s, 4H, CH).
(37) Preparation of compounds **8 – 13** (GP1)
A Schlenk flask was filled with **7** (10 mg, 14.4 µmol), arylboronic acid (2.2 equiv., 31.7 µmol) and K_3PO_4 (12.3 mg, 57.8 µmol), evacuated and purged with argon. A mixture of water/toluene/1,4-dioxane (1:1.8:5.5, 0.5 mL) was added and the resulting suspension degassed with argon for 15 min. Subsequently, $Pd_2(dba)_3$ (0.4 mg, 0.437 µmol) and P(*o*-tol)$_3$ (1.1 mg, 3.61 µmol) were added, and the reaction was heated to 60 °C for 14 h. Upon full conversion of the starting material, the reaction was diluted with CH_2Cl_2 (10 mL) and washed with water (15 mL) three times. The organic phase was dried over $MgSO_4$, the solvent evaporated under reduced pressure and the crude purified by column chromatography (SiO_2, gradient of hexane/ CH_2Cl_2).
(38) Preparation of **14**
In a heat gun dried Schlenk tube under an atmosphere of argon, a mixture of **7** (15 mg, 21.7 µmol), iminodibenzyl (9 mg, 47.7 µmol) and Pd-RuPhos-G4 (1.8 mg, 2.17 µmol) was dissolved in dry 1,4-dioxane (0.5 mL). The resulting mixture was degassed in a stream of argon for 10 min. At this point LiHMDS (0.1 M in THF, 54 µL, 54.2 µmol) was added. After heating to 60 °C for 16 h the reaction mixture was dissolved with CH_2Cl_2 and subsequently washed with water and brine. After drying over $MgSO_4$ and evaporating under reduced pressure, flash column chromatography (SiO_2, hexane/CH_2Cl_2 1:1) afforded the product as a yellow solid. ^{1}H NMR (500 MHz, CD_2Cl_2) δ [ppm] = 7.51 (dd, *J* = 5.4, 3.2 Hz, 8H), 7.14 (ddd, *J* = 8.6, 6.5, 2.4 Hz, 12H), 6.72 (td, *J* = 7.3, 1.2 Hz, 4H), 6.54 (ddd, *J* = 8.7, 7.2, 1.7 Hz, 4H), 6.37 (dd, *J* = 8.4, 1.2 Hz, 4H), 5.61 (s, 4H), 3.67 (s, 8H). HRMS (ESI) m/z: $[M + H]^+$: 921.3700; found 921.3703.
(39) Preparation of **15**
7 (20 mg, 28.9 µmol), $Pd(PPh_3)_4$ (6.4 mg, 5.54 µmol) and CuI (1.0 mg, 5.25 µmol) were suspended in THF/Et_3N (1:1, 1.5 ml). After degassing with argon for 15 min, TIPS-acetylene (150 µL, 578 µmol) was added and the resulting reaction mixture was stirred at 50 °C for 60 h. The green luminescent reaction mixture was quenched by addition of water (5 mL) and extracted three times with CH_2Cl_2 (10 mL). The combined organic layers were dried over $MgSO_4$ and the solvent was evaporated under reduced pressure. The crude was purified by column chromatography (SiO_2, hexane/CH_2Cl_2 4:1 to 1:2). **15** (15 mg, 57%) was obtained as a yellow solid. ^{1}H-NMR (400 MHz, $CDCl_3$) δ [ppm] = 7.54 (dd, *J3* = 5.4 Hz, J4 = 3.2 Hz, 8H, CH), 7.14 (dd, *J3* = 5.4 Hz, *J4* = 3.2 Hz, 8H, CH), 5.60 (s, 4H, CH), 1.34 (s, 36H, CH3), 1.26 (s, 6H, CH); ^{13}C-NMR (100 MHz, $CDCl_3$) δ [ppm] = 157.7, 141.7, 140.2, 127.0, 125.4, 121.3, 107.6, 55.4, 19.1, 11.9. HRMS (ESI) m/z: $[M + H]^+$: 895.4586; found 895.4566.

Supporting Information

Iptycene Containing Azaacenes with Tunable Luminescence

A. Lennart Schleper,[§] Constantin-Christian A. Voll,[§] Jens U. Engelhart and Timothy M. Swager*

Department of Chemistry, Massachusetts Institute of Technology, 77 Massachusetts Avenue, Cambridge MA, 02139, USA

[§] These authors contributed equally

*tswager@mit.edu

Contents

1. General methods S2
2. Synthesis and analytical data S2
3. Additional photophysical data S10
4. References S10

1. General methods

Materials. Acetic acid (AcOH, glacial, Macron), Benzene-1,2,4,5-tetraamine tetrahydrochlorid (technical grade, Sigma Aldrich), *t*BuBrettPhos (97% Sigma Aldrich), *t*BuXPhos (97% Sigma Aldrich), copper(I) iodide (purum, Sigma Aldrich), 4,7-dibromobenzo[*c*]-1,2,5-thiadiazole (95%, Sigma Aldrich), dichloromethane (CH_2Cl_2, 99.5%, containing amylene as stabilizer, Sigma Aldrich), 3,5-dimethoxyphenylboronic acid (95%, Sigma Aldrich), dimethyl sulfoxide (DMSO, anhydrous, 99.9%, Sigma Aldrich), hexane (Macron), 2-methoxybenezeneboronic acid (Alfa Aesar), 4-methoxybenzeneboronic acid (95%, Sigma Aldrich), 3-methoxythiophen-2-boronic acid pinacol ester (Sigma Aldrich), nitric acid (HNO_3, fuming, 90%, Sigma Aldrich), phenylboronic acid (TCI America), potassium phosphate (K_3PO_4, tribasic, Sigma Aldrich), RuPhos (95% Sigma Aldrich), silica gel (SiO_2, technical grade, Sigma Aldrich), tetrakis(triphenylphosphine)palladium ($Pd(PPh_3)_4$, 99%, Sigma Aldrich), thianaphthene-2- boronic acid (Sigma Aldrich), 2,5-thiophendiboronic acid (Sigma Aldrich), trifluoroacetic anhydride (TFAA, 99%, Sigma Aldrich), trifluoromethanesulfonic acid (TFMS, reagent grade, Sigma Aldrich), (tri-*iso*-propylsilyl)acetylene (TIPS-acetylene, 97%, Sigma Aldrich), tris(dibenzylideneacetone)dipalladium ($Pd_2(dba)_3$, TCI America), tri(*o*-tolyl)phosphine ($P(o\text{-tol})_3$, Sigma Aldrich), XPhos (97%, Sigma Aldrich) and zinc powder (purum, Sigma Aldrich) were purchased commercially and used without any further purification. 9,10-dihydro-9,10-ethanoanthracene-11,12-diole (**3**) was already present in the group. Dry solvents were obtained from a solvent purification system and stored under argon atmosphere. High Resolution Mass Spectrometry (HRMS) experiments were executed with a Bruker Daltonics APEXIV 4.7 Tesla Fourier Transform Ion Cyclotron Resonance Mass Spectrometer. Nuclear Magnetic Resonance (NMR) experiments were carried out using a Varian Mercury- 300, a Bruker Avance III-400 or a JEOL ECZ-500 NMR. Optical Measurements were carried out in a quartz cuvette (1cm x 1cm) filled with 3 ml hexane and a solution of the optical active compound in hexane/CH_2Cl_2. Absorption spectra were collected with a Cary 4000 UV-Vis spectrophotometer from Agilent Technologies and fluorescence spectra were collected with a Jobin Yvon FL3-21 system.

2. Synthesis and analytical data

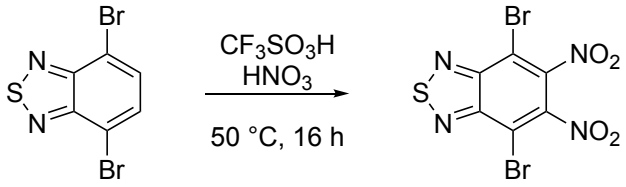

According to a literature procedure,[1] TFMS (26.0 mL, 294 mmol) was added under stirring and ice cooling dropwise to fuming nitric acid (3.4 mL, 81.5 mmol). Next, 4,7-dibromobenzo[*c*][1,2,5]thiadiazole (7.5 g, 25.5 mmol) was added in small portions over 20 min. The reaction mixture was stirred at 50°C for 16 h, quenched by pouring on ice water and neutralized by addition of 4M NaOH (95 mL). The reaction mixture was filtered and the precipitate washed with

water and recrystallized from ethanol (300 mL). The product **5** (5.25 g 13.6 mmol, 54%) was obtained as off-white crystals. Further product (920 mg, 2.4 mmol, 9%) was obtained as light brown crystals by

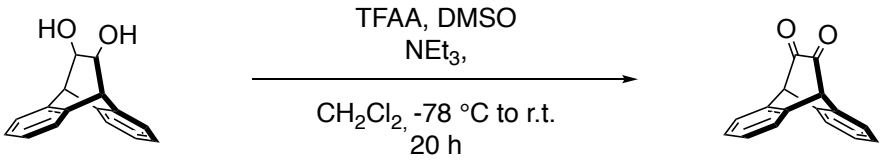

3 **4**

evaporating the mother lye and recrystallizing the residue.

Under argon atmosphere, DMSO (3.8 mL, 53.4 mmol) was dissolved in CH_2Cl_2 (215 mL) and cooled to -78°C where TFAA (6.5 mL, 45.9 mmol) was added over a period of 15 min. Then a solution of diol **3** (3.6 g, 15.1 mmol) in CH_2Cl_2 (81 mL) and DMSO (40.5 mL) was added over 30 min. After stirring for 1 h at -78°C, NEt_3 (14.6 mL, 105 mmol) the reaction was slowly warmed to room temperature over the course of 20 h. At this point, the reaction was quenched by the addition 2M hydrochloric acid (540 mL). The aqueous phase was extracted with CH_2Cl_2 (100 mL) eight times and the combined organic extracts were washed with water and dried over $MgSO_4$. Next, the solvent was evaporated and the residue was purified by column chromatography (SiO_2, CH_2Cl_2). The product (**4**, 2.86 g, 12.2 mmol, 80%) was obtained as yellow solid.

NMR: ^{1}H (400 MHz, $CDCl_3$) δ [ppm] = 7.48 (dd, *J3* = 5.5 Hz, *J4* = 3.2 Hz, 4H, CH), 7.38 (dd, *J3* = 5.5 Hz, *J4* = 3.2 Hz, 4H, CH), 5.00 (s, 2H, CH).

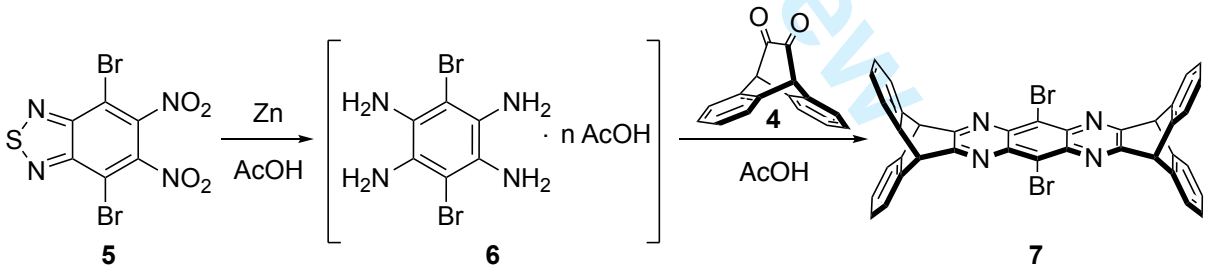

5 **6** **7**

The optimized reaction was carried out in a 20 ml vial, containing zinc powder (470 mg, 7.2 mmol) suspended in AcOH (3.5 mL). Under stirring **5** (138 mg, 358 µmol) was added and the reaction mixture heated to 60°C for 60 min. The reduced colorless intermediate **6** was separated from the zinc powder by filtration through a pad of celite and added dropwise to a solution of **4** (61 mg, 260 µmol) in AcOH (1.5 mL) over 60 min. Immediately, a yellow precipitate was formed. The solution was stirred for further 60 min and then extracted several times with CH_2Cl_2 (20 mL) until the organic phase was colorless. The combined organic layers were washed with an aqueous $NaHCO_3$ solution (100 mL) and

water (100mL). After evaporation of the solvent, the crude product was purified via column chromatography (SiO_2, hexane/ CH_2Cl_2 3:1 → 0:1). The product (**7**, 65 mg, 93.8 µmol, 72%) was obtained as yellow powder.

NMR: 1H (400 MHz, CDCl3) δ [ppm] = 7.59 (dd, *J3* = 5.4 Hz, *J4* = 3.2 Hz, 4H, CH), 7.17 (dd, *J3* = 5.4 Hz, *J4* = 3.2 Hz, 4H, CH), 5.84 (s, 4H, CH).

Preparation of Compounds 8 – 13

Preparation of compounds **8 – 13** (GP1): A Schlenk flask was filled with **7** (10 mg, 14.4 µmol), arylboronic acid (2.2 equiv., 31.7 µmol) and K_3PO_4 (12.3 mg, 57.8 µmol), evacuated and purged with argon. A mixture of water/toluene/1,4-dioxane (1:1.8:5.5, 0.5 mL) was added and the resulting suspension degassed with argon for 15 min. Subsequently, $Pd_2(dba)_3$ (0.4 mg, 0.437 µmol) and P(*o*-tol)$_3$ (1.1 mg, 3.61 µmol) were added, and the reaction was heated to 60 °C for 14 h. Upon full conversion of the starting material, the reaction was diluted with CH_2Cl_2 (10 mL) and washed with water (15 mL) three times. The organic phase was dried over $MgSO_4$, the solvent evaporated under reduced pressure and the crude purified by column chromatography (SiO_2, gradient of hexane/ CH_2Cl_2).

Preparation of **8**: According to GP1, **7** (10 mg) was coupled with 3,5- dimethoxybenzeneboronic acid (5.5 mg). The crude was purified by column chromatography (SiO_2, hexane/ CH_2Cl_2 2:1 → 0:1). The product (**11**, 11.6 mg, 14.4 µmol, 99%) was obtained as a yellow powder. ^{1}H-NMR (300 MHz, $CDCl_3$) δ [ppm] = 7.47 (dd, *J3* = 5.4 Hz, *J4* = 3.2Hz, 8H, CH),7.10 (dd, *J3*=5.4Hz, *J4* =3.2 Hz, 8H, CH),6.65 (t, *J*=2.3 Hz, 2H, CH), 6.62 (d, *J* = 2.3 Hz, 4H, CH), 5.58 (s, 4H, CH), 3.85 (s, 12H, CH3). HRMS (ESI) m/z: $[M + H]^+$: 807.2966; found 807.2954.

Preparation of **9:** According to GP1, **7** (10 mg) was coupled with phenylboronic acid (3.9 mg). The crude was purified by column chromatography (SiO_2, hexane/CH_2Cl_2 3:1 → 0:1). The product (**9**, 9.9 mg, 14.4 µmol, 99%) was obtained as a yellow powder. ^{1}H-NMR (300 MHz, $CDCl_3$) δ [ppm] = 7.59 – 7.58 (m, 2H) 7.57 (d, *J* = 1.8 Hz, 4H, CH), 7.51- 7.50(m, 4H), 7.47 (dd, *J3* =5.4Hz, J4 =3.2Hz, 8H, CH), 7.09 (dd, *J*3 =5.4Hz, *J4* =3.2Hz, 8H, CH), 5.54 (s, 4H, CH). HRMS (ESI) m/z: $[M + H]^+$: 687.2543; found 687.2539.

Preparation of **10:** According to GP1, **7** (10 mg) was coupled with 2- methoxybenzeneboronic acid (4.8 mg). The crude was purified by column chromatography (SiO_2, hexane/CH_2Cl_2 3:1 → 0:1). The product (**10**, 7.1 mg, 9.5 µmol, 66%) was obtained as a yellow powder. ^{1}H-NMR (300 MHz, CD_2Cl_2) δ [ppm] = 7.60 – 7.46 (m, 10H), 7.19 – 7.09 (m, 14H), 5.54 (s, 4H, CH), 3.54 (d, *J* = 13.5 Hz, 6H, CH) HRMS (ESI) m/z: $[M + H]^+$: 747.2755; found 747.2745.

Preparation of **11:** According to GP1, **7** (10 mg) was coupled with 4- methoxybenzeneboronic acid (4.8 mg). The crude was purified by column chromatography (SiO_2, hexane/CH_2Cl_2 2:1 → 0:1). The product (**12**, 10.7 mg, 14.4 µmol, 99%) was obtained as a yellow powder. ^{1}H-NMR (300 MHz, $CDCl_3$) δ [ppm] = 7.49 – 7.47 (m, 8H), 7.46 (d, *J* = 1.6 Hz, 4H, CH), 7.11 – 7.08 (m, 12H), 5.57 (s, 4H, CH), 4.00 (s, 6H, CH3). HRMS (ESI) m/z: $[M + H]^+$: 747.2755; found 747.2736.

Preparation of **12:** GP1 was carried out with **7** (10 mg) and 3-methoxythiophen-2- boronic acid pinacol ester (7.6 mg). The crude product was purified by column chromatography (SiO_2, hexane/CH_2Cl_2 2:1 → 0:1, including 10% NEt_3). The product (**14**, 7.5 mg, 9.9 µmol, 69%) was obtained as a yellow powder. HRMS (ESI) m/z: $[M + H]^+$: 759.1883; found 759.1900. ^{1}H NMR (500 MHz, CD_2Cl_2) δ [ppm] = 7.61 (m, 5H), 7.53 (9H, m), 7.14 (br, 13H), 5.63 (4H, br), 3.70, br). Due to low solubility, only a poor NMR spectrum could be obtained.

Preparation of **13:** According to GP1, **7** (10 mg) was coupled with thianaphthene-2- boronic acid (5.7 mg). The crude was purified by column chromatography (SiO_2, hexane/CH_2Cl_2 3:1 → 0:1). The product (**13**, 7.5 mg, 9.4 µmol, 65%) was obtained as an orange powder. Due to poor solubility, only a poor NMR spectrum could be obtained. HRMS (ESI) m/z: $[M + H]^+$: 799.1985; found 799.1967.

2.2 Analytical data

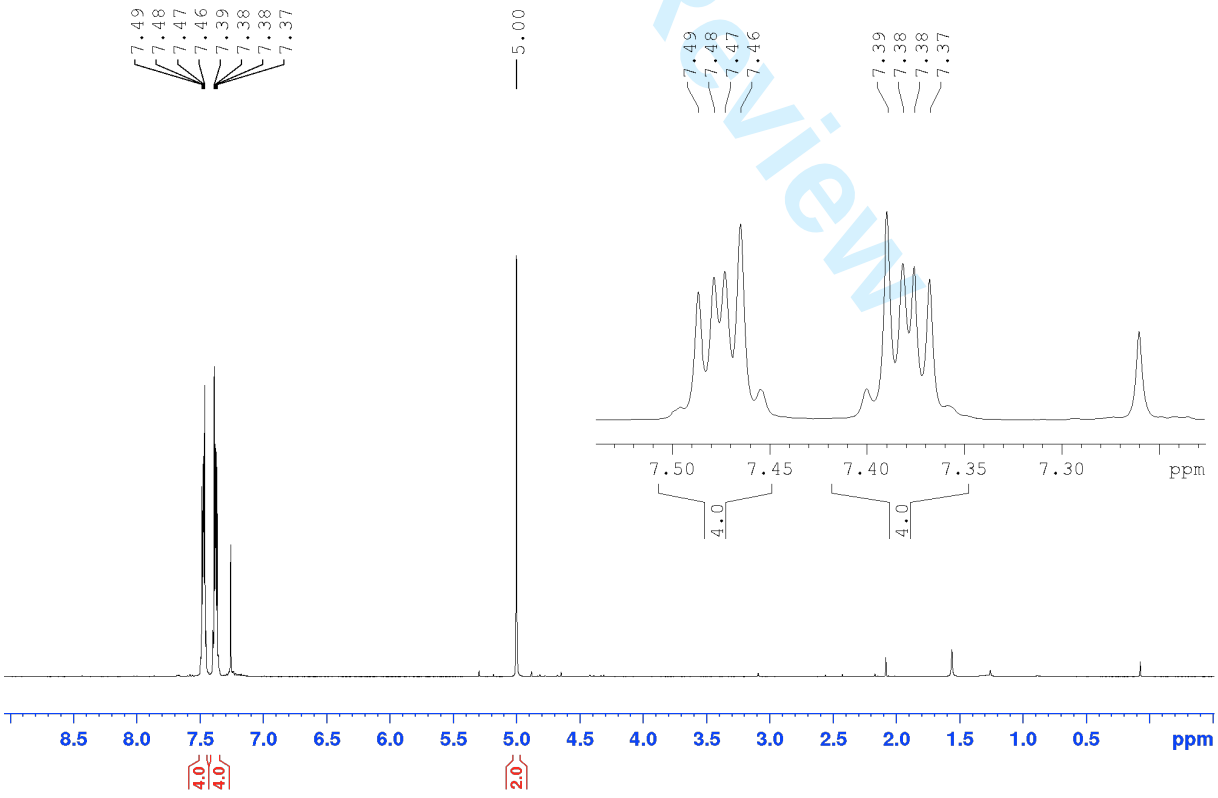

Figure S1: ^{1}H NMR of compound **4** in CD_2Cl_2.

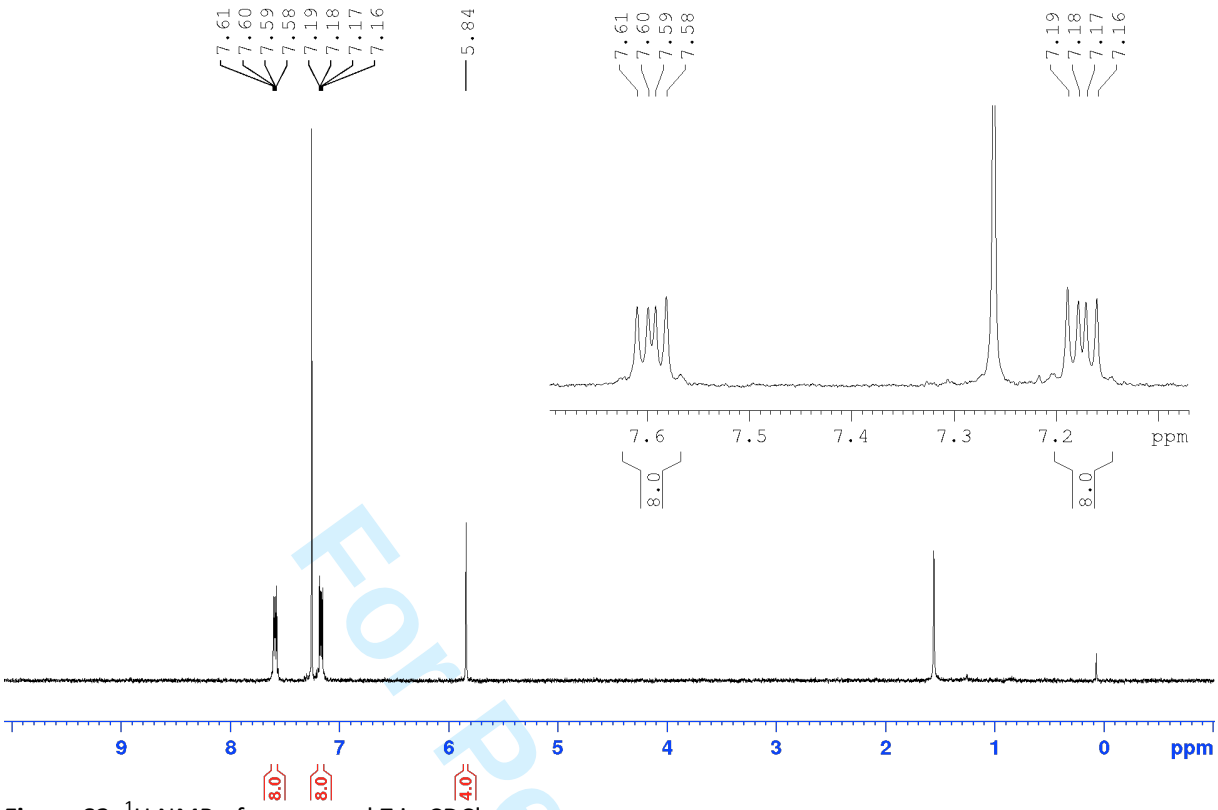

Figure S2: ^{1}H NMR of compound **7** in $CDCl_3$.

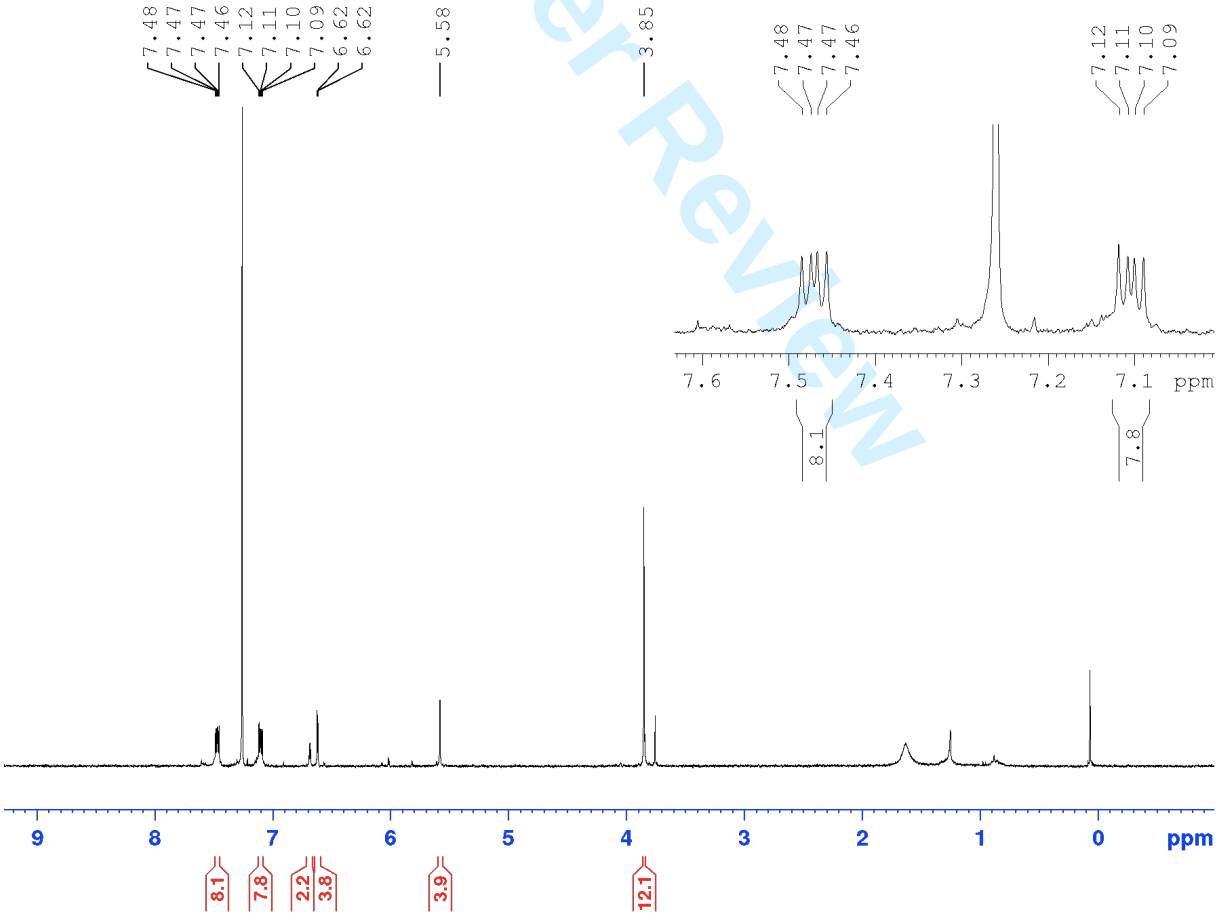

Figure S3: ^{1}H NMR of compound **8** in $CDCl_3$.

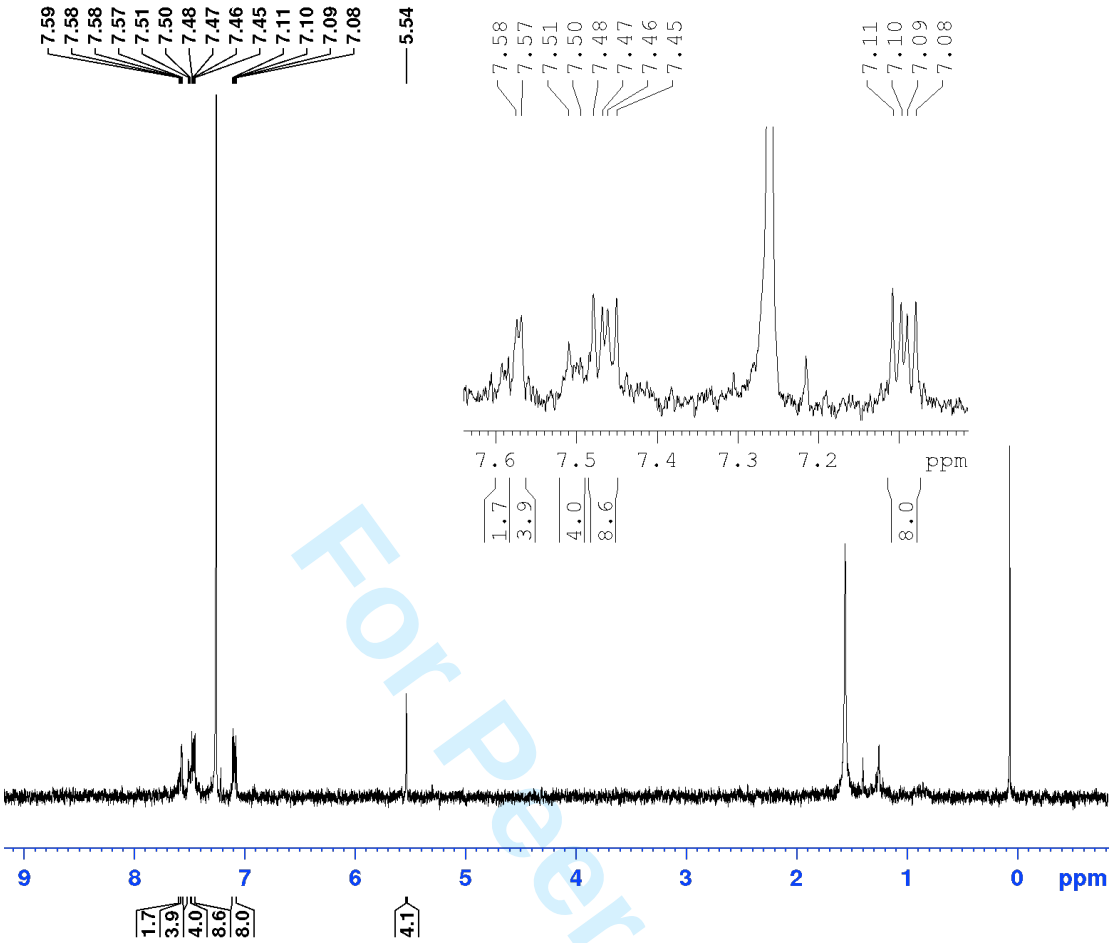

Figure S4: ^{1}H NMR of compound **9** in $CDCl_3$.

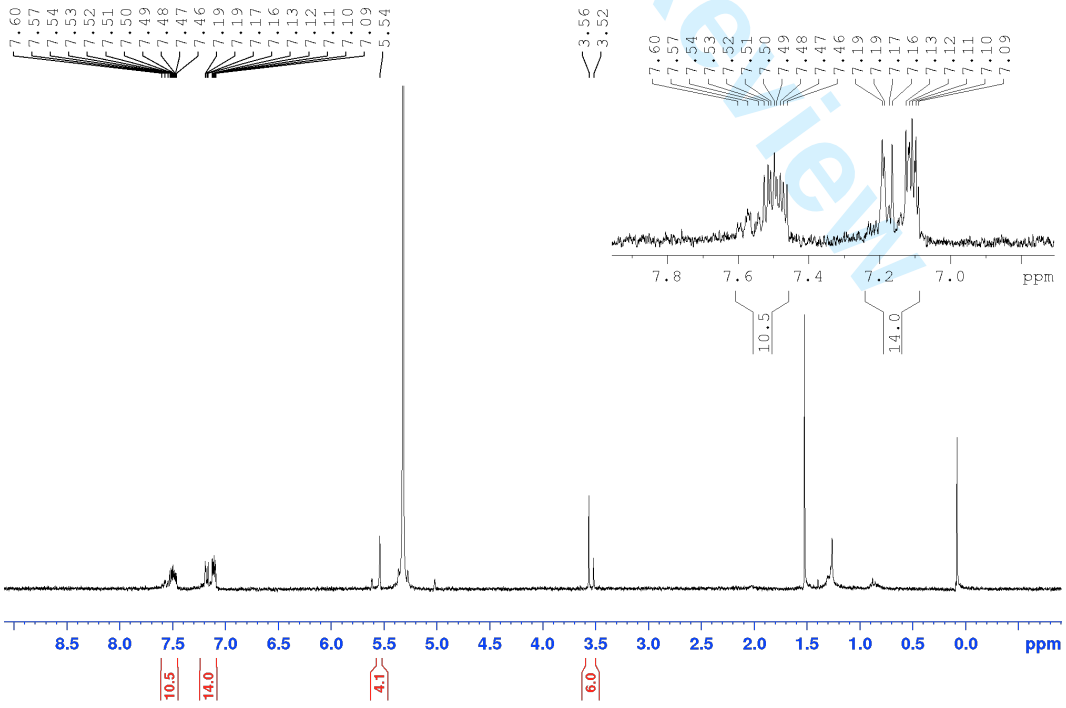

Figure S5: ^{1}H NMR of compound **10** in CD_2Cl_2.

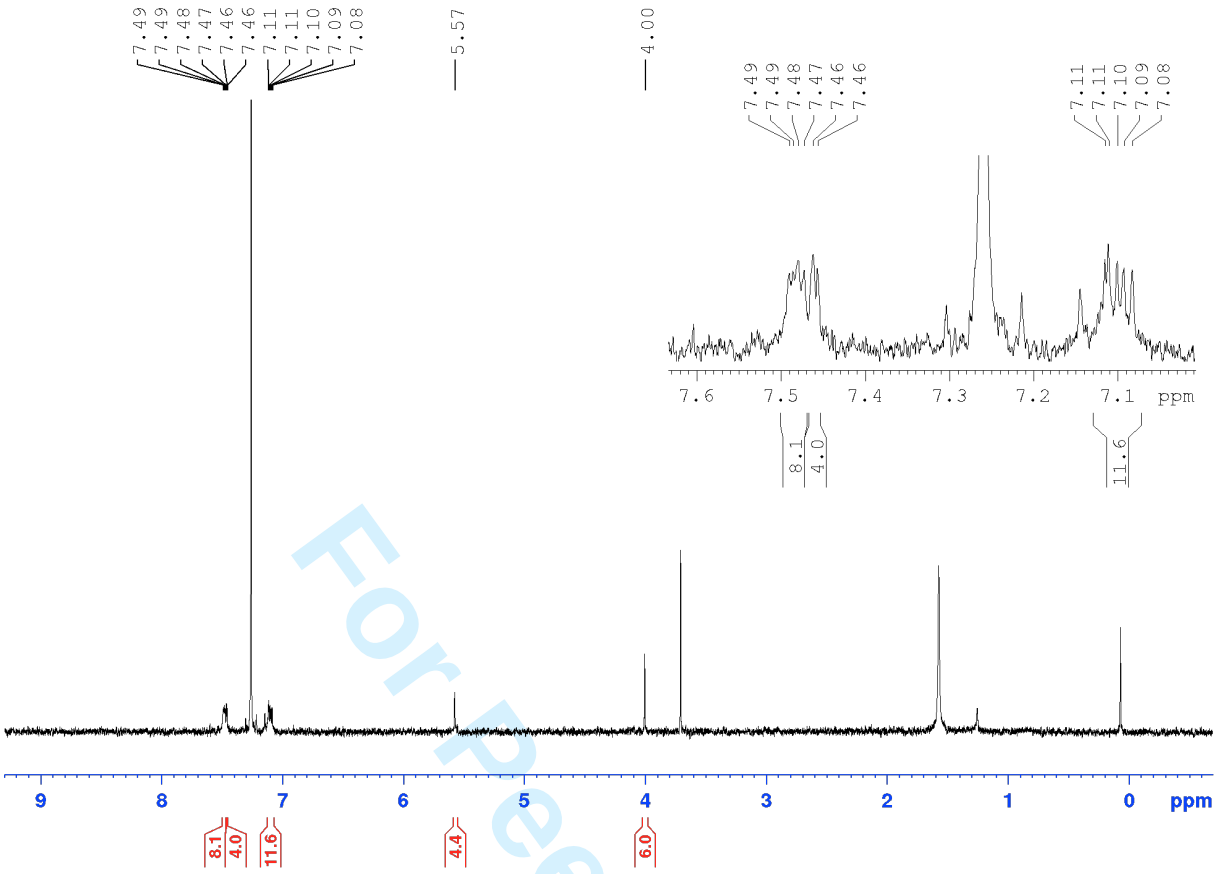

Figure S4: ^{1}H NMR of compound **11** in $CDCl_3$.

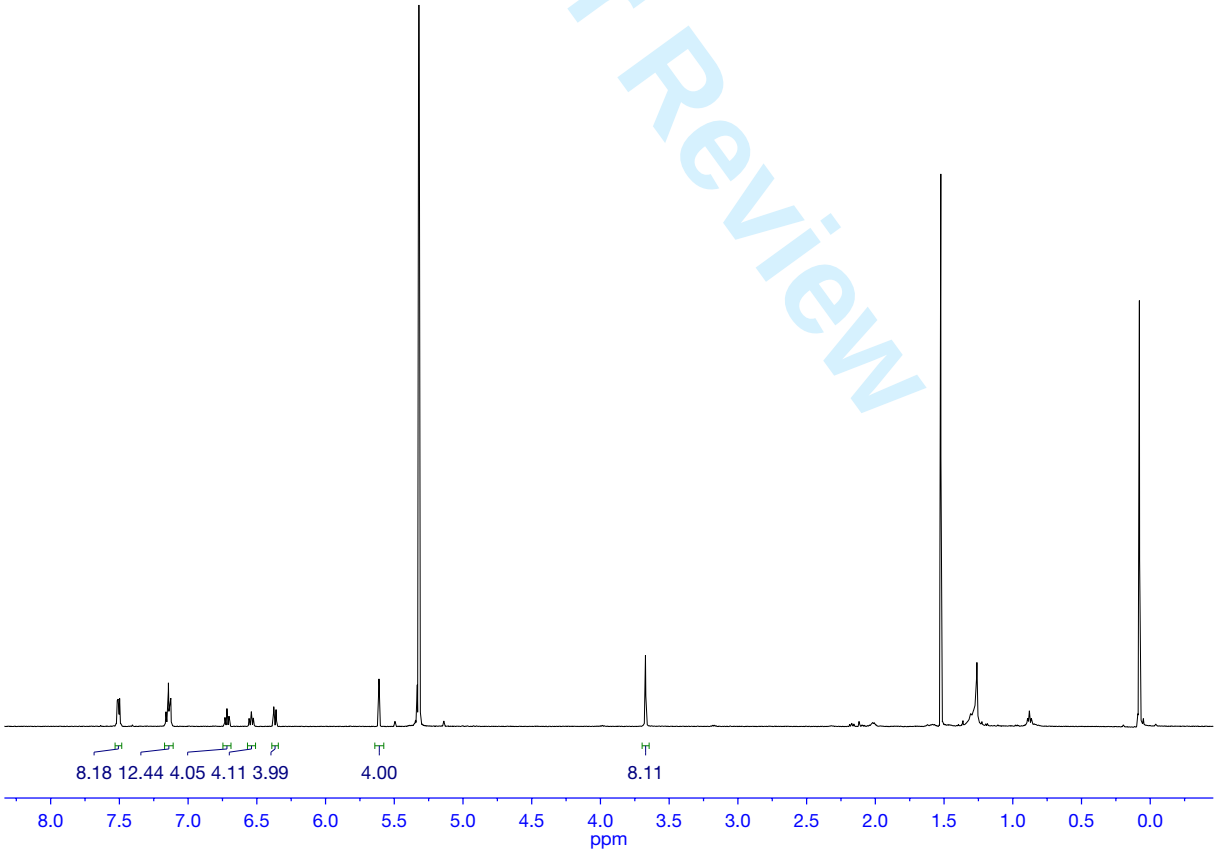

Figure S7: ^{1}H NMR of compound **14** in CD_2Cl_2.

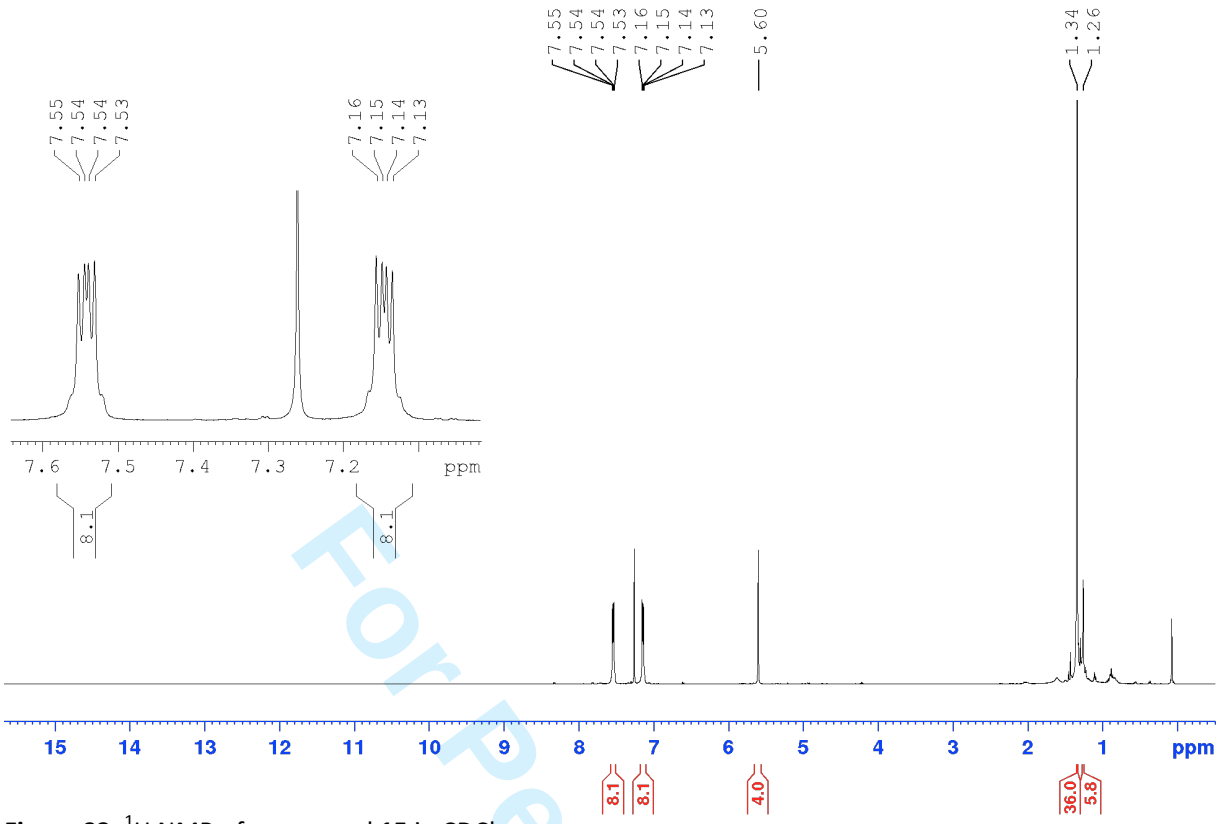

Figure S8: ^{1}H NMR of compound **15** in $CDCl_3$.

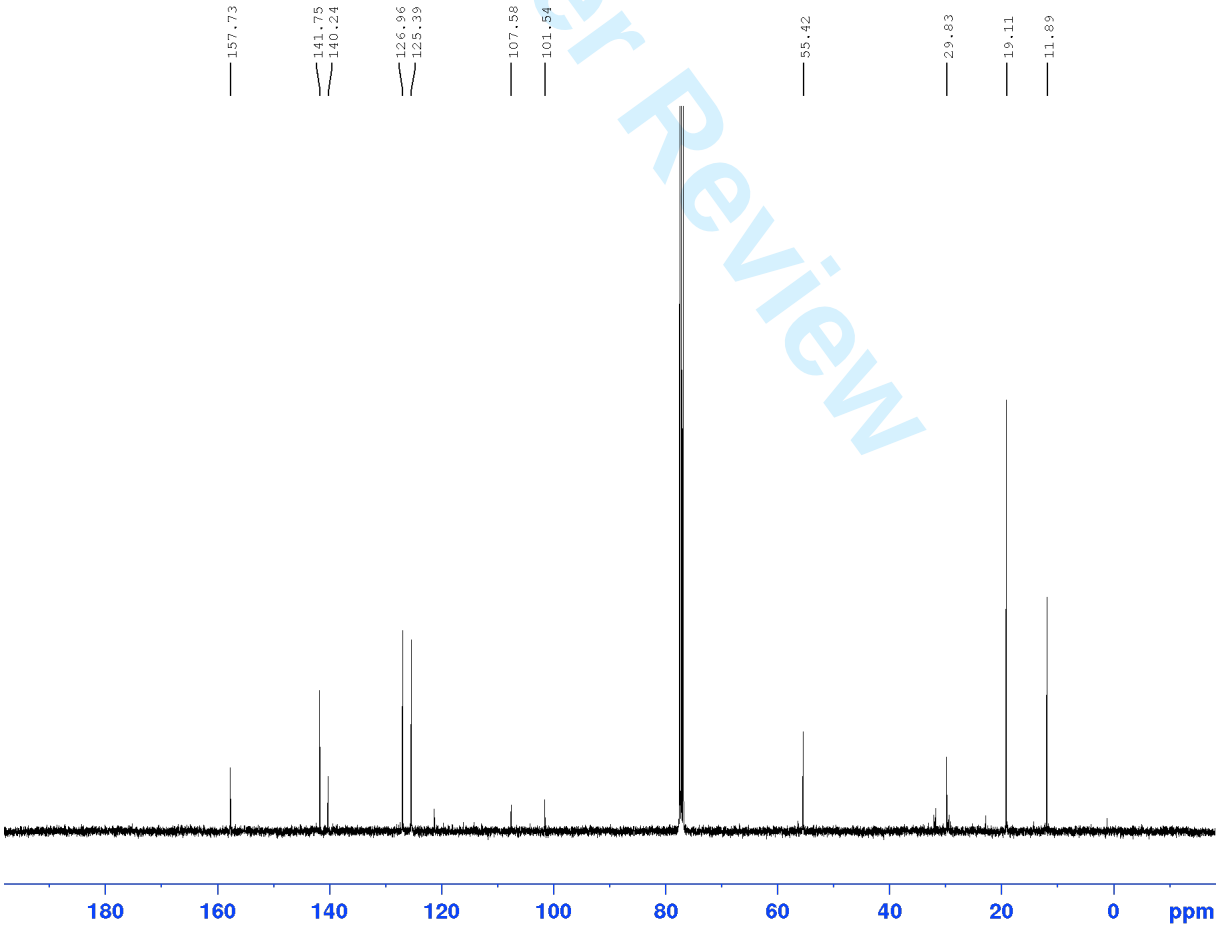

Figure S9: ^{13}C {^{1}H} NMR of compound **15** in $CDCl_3$.

3. Additional photophysical data

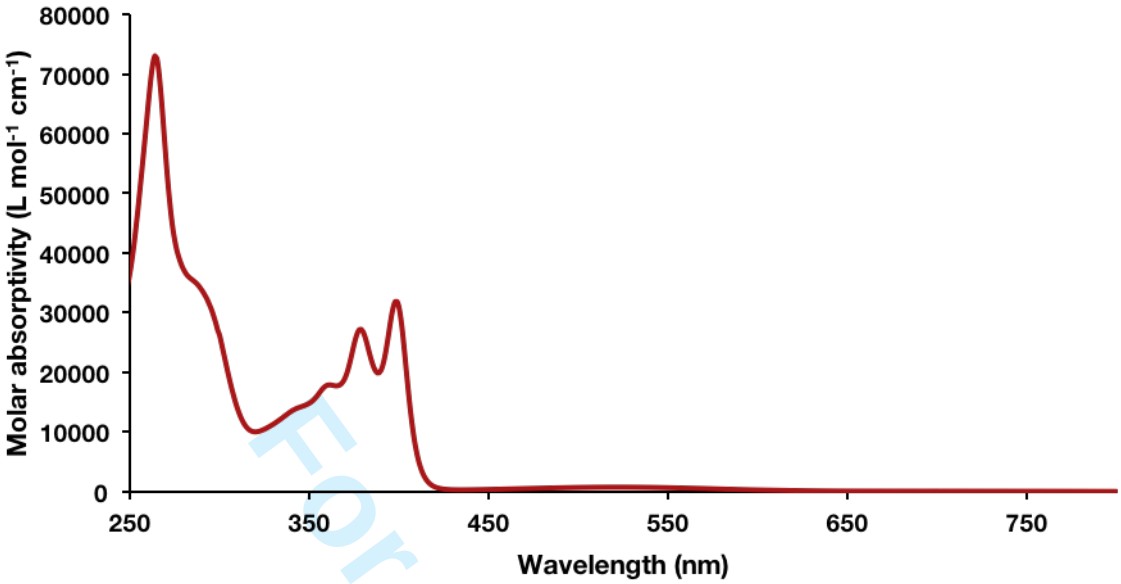

Figure S10: Absorption spectrum of **14** in CH_2Cl_2.

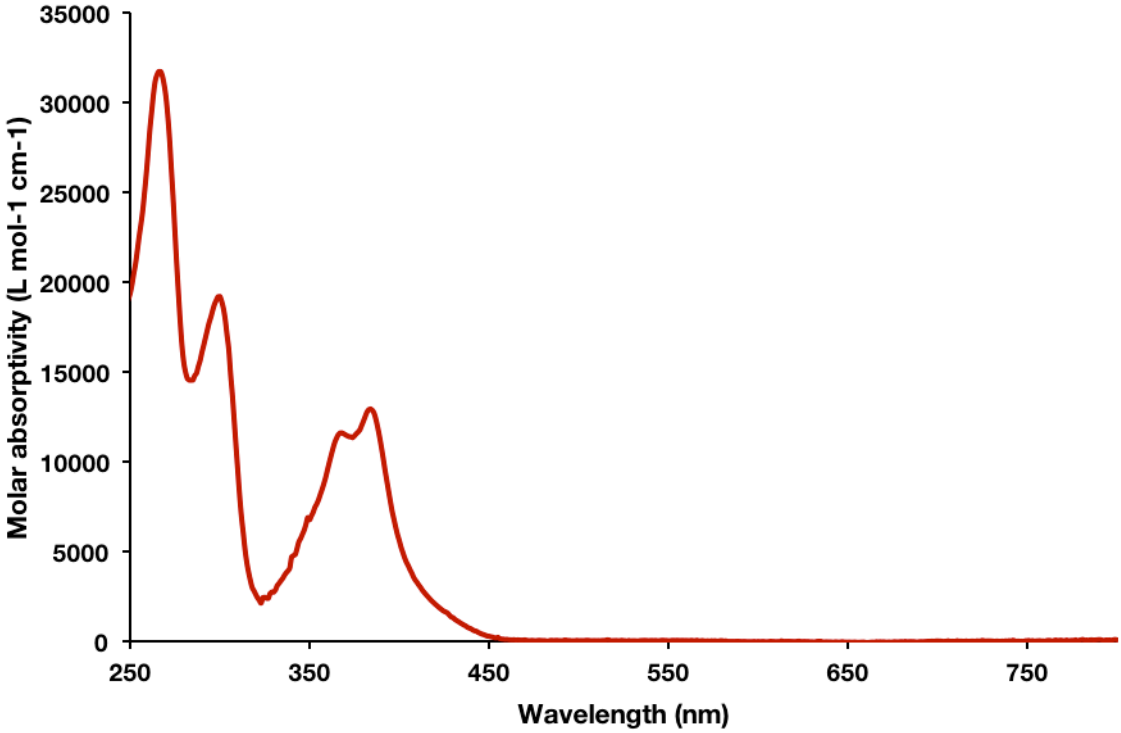

Figure S11: Absorption spectrum of **8** in hexane.

4. References

[1] E. Wang, L. Hou, Z. Wang, S. Hellström, W. Mammo, F. Zhang, O. Inganäs, M. R. Andersson, *Org. Lett.* **2010**, *12*, 4470–4473.

Iptycene Containing Azaacenes with Tunable Luminescence

A. Lennart Schleper[§]
Constantin-Christian A. Voll[§]
Jens U. Engelhart
Timothy M. Swager*

Department of Chemistry, Massachusetts Institute of Technology, 77 Massachusetts Avenue, Cambridge MA, 02139, USA
tswager@mit.edu

[§] These authors contributed equally

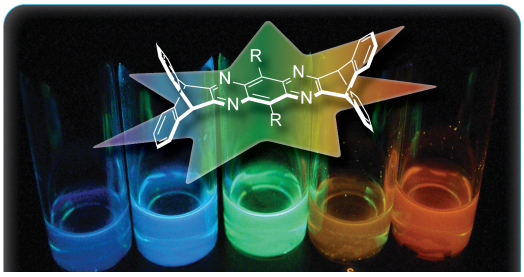

Received:
Accepted:
Published online:
DOI:

Abstract An optimized route toward iptycene-capped, *p*-dibromo-quinoxalinophenazine **7** was developed, increasing the yield significantly from literature procedures. New iptycene containing symmetrical azaacenes were synthesized from this intermediate using Suzuki-Miyaura cross-coupling and their photophysical properties were evaluated. Tuning the substituents allows modulating emission wavelengths across the visible spectrum. Substitution with 3-methoxy-2-methylthiophene (**12**) exhibits a quantum yield of 35%. The (triisopropylsilyl)acetylene product **15** has a quantum yield of 38% and serves as a model compound for the synthesis of polymers based on this electrooptically-active molecular motif.

Key words N-heteroiptycene, Suzuki-Miyaura cross-coupling, Sonogashira coupling, pyrazinoquinoxaline, luminescence

In recent years, there has been an immense interest in organic materials for OLEDs, OFETs and PVs, encouraged by the ease of tunability through design and solubility compared to inorganic counterparts, which is conducive to large-scale printing techniques.[1,2] OLEDs, as an example, initially struggled with efficiency because upon electrochemical excitation, singlet and triplet excitons are formed in a 1:3 statistical ratio.[3] Since only the radiative decay from singlet excitons is quantum chemically fully allowed and the long-lived triplet excitons usually relax through non-radiative processes, internal electroluminescent quantum efficiency (η_{int}) of most organics is limited to 25%. Phosphorescent materials and delayed fluorescence have been investigated as triplet harvesting strategies. Most of these materials incorporate heavy metals and have been shown to achieve η_{int} values that are essentially 100%. However, their use is constrained by cost, the limited stability of blue emitters, and triplet-triplet annihilation at high current densities.[4–6] Emissive stable radicals have also been considered, but there are currently only a limited number of structures suitable for this purpose and quantum efficiencies have thus far been low.[7,8] Recently high emission efficiencies from thermally activated delayed fluorescence (TADF) have been reported and this method is emerging as a promising approach to create efficient OLEDs.[9] Indeed this method tends to outperform the up-conversion of triplets to singlet excitons by triplet-triplet annihilation.[10–12] TADF requires the energetic proximity of the S_1 and T_1 state and the first-order mixing coefficients between singlet and triplet states are inversely proportional to the singlet-triplet gap (ΔE_{ST}).[13] This small ΔE_{ST} allows fast intersystem crossing for the thermal equilibration of triplet and singlet excitons. Electroluminescence with η_{int} approaching 100% have been realized through TADF.[9,14] There are two classes of TADF materials that meet the electronic requirements of a low ΔE_{ST}. A torsion angle between donor and acceptor moieties[9,15,16] or having the donor-acceptor groups in homoconjugation, both provide mechanisms to produce segregated HOMO and LUMO states that lower the exchange energy and give rise the small energy difference.[17] In fact, another promising approach for OLEDs and other optical applications involves the spatial segregation of FMOs. In this context we were interested in investigating cruciforms comprising two perpendicular π–conjugated linear units connected by a central aromatic core and thereby can reduce HOMO and LUMO orbital overlap.[18–22]

spacious wings to avoid π–stacking

electron–poor core (LUMO) – acceptor

electron–rich substitutents (HOMO) – donor

Figure 1: Generic target structures targeted in this publication.

We postulated the generic structure shown in Figure 1 to display favorable optical properties. The electron-deficient pyrazinoquinoxaline core will have little HOMO-LUMO orbital overlap with a relatively bulky electron donor that is forced to adopt a twisted conformation.[23,24] The three-dimensional structurally rigid iptycene wings minimize the typical tendency of azaacenes for π-stacking that can lead to self-quenching and reduced quantum yields.[25,26] The isolated phenyl groups of the iptycene wings are not expected to contribute significantly to the HOMO or LUMO.[27]

We targeted a modular synthetic route for symmetric azaacenes and envisioned **7** as a valuable key intermediate because the lateral aryl bromides allow functionalization through cross-coupling reactions. The diketone intermediate **4** was synthesized as shown in Scheme 1, through adaptation of a literature procedure that involves Diels-Alder reaction of anthracene with vinylene carbonate, followed by a basic hydrolysis and a Swern oxidation.[28]

Scheme 1. Synthetic procedure for the synthesis of intermediate **7**.

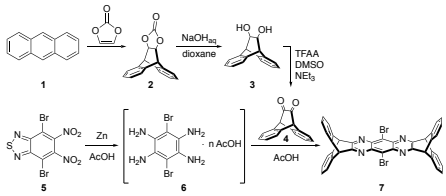

The condensation of **4** was complicated by the fact that 3,6-dibromobenzene-1,2,4,5-tetraamine (**6**) is unstable and has to be prepared *in situ*. Literature procedures for the reduction of 4,7-dibromo-5,6-dinitrobenzo[*c*][1,2,5]thiadiazole (**5**) followed by condensation to a diketone are generally low yielding (20 and 47% for related structures),[29,30] and as a result we decided to optimize the reaction cascade. Following the established literature procedure provided **7** in 33% yield (Entry 2, Table 1). Other reaction conditions such as varying the temperature, zinc-activation by hydrochloric acid, increasing the amount of zinc or the use of hydrochloric acid, instead of acetic acid, did not increase the yield of the reaction (Entries 1, 3 – 6, Table 1). Analysis of the reaction mixture revealed a considerable amount of residual diketone **4**, thus encouraging the use of an excess of **5**. Yields improved up to 65% when 1.38 equivalents of **5** were utilized (Entry 8, Table 1).

Table 1: Reaction optimization for the synthesis of **7**

Entry	T (°C)[a]	Activated Zinc[b]	Acid	Zinc (equiv.)	**5** (equiv.)	Yield (%)
1	50	No	AcOH	20	0.50	trace
2	60	No	AcOH	20	0.50	33[c]
3	70	No	AcOH	20	0.50	trace
4	60	Yes	AcOH	20	0.50	trace
5	60	No	HCl	20	0.50	trace
6	60	No	AcOH	200	0.50	trace
7	60	No	AcOH	20	1.25	61[c]
8	60	No	AcOH	20	1.38	65[c]
9	60	No	AcOH	20	1.50	57[c]
10	60	No	AcOH	20	1.38	72[c]

[a] Temperature used for reduction of **5** to **6** [b] Zinc activation by HCl [c] isolated yield

Having the tetraamine **6** in excess, however, increases the likelihood of mono-condensation hence the order of addition was reversed. Slowly adding the amine to a solution of the diketone in acetic acid over 1 h furthermore raised the yield to 72% (Entry 10, Table 1). Despite the promising increase in yield, we encountered issues in scaling up the reaction and diminished yields were observed at scales more than 60 mg of **4**.

Having optimized the first reaction cascade, we endeavored to introduce donor groups to **7** through cross-coupling reactions. We surveyed both Stille and Suzuki-Miyaura couplings, and converged on the latter based upon higher yields whilst avoiding toxic tin reagents. Reaction optimization with (3,5-dimethoxyphenyl)boronic acid revealed that cross-coupling to **7** could be achieved in 99% yield using $Pd_2(dba)_3$/P(*o*-tol)$_3$ as the catalyst at 60 °C. Other catalysts such as $Pd(PPh_3)_4$, the addition of CuI, Pd-XPhos-G2 or $Pd(dppf)Cl_2$ resulted in low to moderate yields (Table 2).

Table 2: Optimization of Suzuki-Miyaura cross-coupling

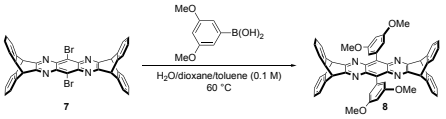

Entry	Catalyst	CuI (equiv.)	Yield (%)
1	$Pd(PPh_3)_4$	—	trace
2	$Pd(PPh_3)_4$	0.2	trace
3	Pd-XPhos-G2	—	47[a]
4	$Pd(dppf)Cl_2$	—	54[a]
5	$Pd_2(dba)_3$/P(*o*-tol)$_3$	—	99[a]

[a] isolated yield

The optimized reaction conditions were applied to a variety of (hetero)aryl boronic acids and the C-C cross-coupling products **9** – **13** could be obtained in yields ranging from 65 to 99% (Figure 2).

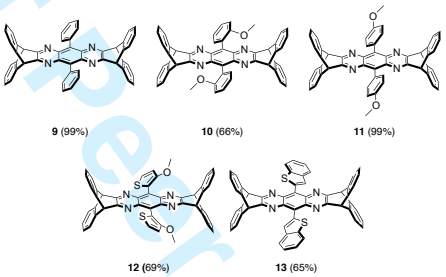

Figure 2: Substrate scope of aryl boronic acid coupling with **7**.

We furthermore attempted to extend the scope to include Pd-catalyzed *N*-arylation with carbazole in order to introduce stronger donors. Unfortunately, initial attempts using a variety of ligands (XPhos, *t*BuBrettPhos, RuPhos or *t*BuXPhos) only produced unreacted and reduced forms of **7**. However, the *N*-arylation with iminodibenzyl, which is known to be a better nucleophile than carbazole,[31] proceeded smoothly to give **14** in 56% yield using the Buchwald precatalyst Pd-RuPhos-G4 (Scheme 2).

Deleted: 3

Deleted: 2017-05-062017-05-05

Scheme 2: *N*-arylation reaction of iminodibenzyl with **7**.

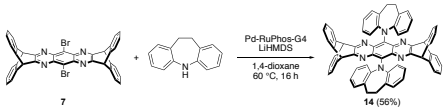

These promising coupling results with aryl bromides also encouraged us to synthesize a (triisopropylsilyl)acetylene product (**15**) via a Sonogashira reaction catalyzed by $Pd(PPh_3)_4$ and CuI in 57% yield (Scheme 3). This compound serves as a model compound for a hypothetical acetylene-linked polymer of **7**. The yield of the Sonogashira reaction in this case is too low to be of utility for the synthesis of polymers, which require near quantitative yields. We note that **15** has very recently been synthesized by Bunz and co-workers through a different synthetic route.[32]

Scheme 3: Sonogashira coupling of **7** with (triisopropylsilyl)acetylene to form **15**.

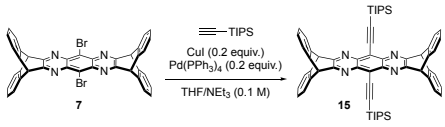

Photophysical Characterization

We were interested to determine if these materials displayed desirable optical properties, including TADF. Representative absorption spectra of the compounds **9-13** are shown in Figure 3. All of the compounds display vibronic fine structure with peaks that are summarized in Table 3. The broad tails at longer wavelength are suggestive of charge transfer character.

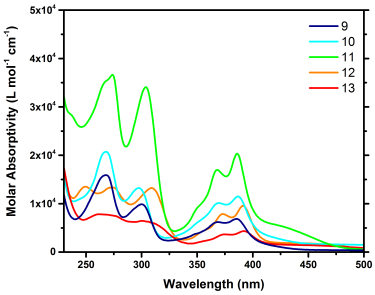

Figure 3: Absorption spectra with molar absorptivity for **9 – 13** in hexane.

To determine if this class of compounds display TADF behavior, we measured the quantum yields in both deoxygenated and oxygen-containing solvents. In TADF systems, triplet states contribute to a delayed component, which renders the compounds susceptible to quenching by oxygen.[33,34] An increase in quantum yield in an oxygen-free solvent is therefore an indication of TADF. As shown in Figure 4, compounds **9-13** were emissive, however saturating the solutions with oxygen did not significantly affect the quantum yield, thereby suggesting that these compounds are not TADF active or have a sufficient lifetime because of rapid non-radiative processes. Compound **14**, which has a stronger donor in the iminodibenzyl group, was only weakly emissive as a result of a weak charge transfer band (Figure S10). Nevertheless, the absorption and emission compounds produced impressively cover essentially the whole visible spectrum.

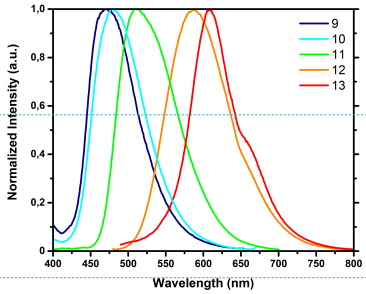

Figure 4: Emission spectra of compounds **9 – 13** in hexane.

Table 3: Optical properties of compound **9** – **15**, measured in hexane.

Compound	λ_{max} (emis)	QY (%)	λ_{max} (abs)
9	470	2.2 x 10^{-3}	268, 300, 367, 385
10	478	0.06	268, 397, 368, 387
11	510	0.07	274, 303, 368, 386
12	586	0.35	248, 274, 309, 373, 397
13	608	0.11	266, 301, 374, 393
14	—	—	265, 360, 378, 400, 522
15	466, 495	0.29 (0.38)[a]	275, 307, 378, 400, 427, 454

[a] degassed by bubbling argon through solution

The (Triisopropylsilyl)acetylene product **15** shows several well-defined absorption maxima as shown in Figure 5. The compound is emissive with a maximum at 466 nm with a pronounced shoulder peak at 495 nm, to give a visibly green emission. The quantum yield was 38% in degassed hexane but decreased to 29% after oxygen exposure. This suggests the presence of long lived excited states, most likely triplet states, that are quenched by O_2.

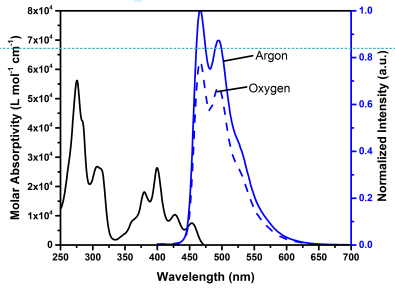

Figure 5: Photophysical characterization of **15**, measured in hexane.

Deleted: 3

Deleted: 4

Deleted: 4

Moved (insertion) [1]

Deleted:

Deleted: 4

Deleted: 8

Deleted: 1

Deleted: 4

Deleted: A_{max}

Formatted: Font:7.5 pt

Deleted: 4

Moved up [1]: Figure 4: Emission spectra of compounds **9 – 13** in hexane.

Deleted: *<sp>*

Formatted: Font:7.5 pt

Deleted: 2017-05-062017-05-05

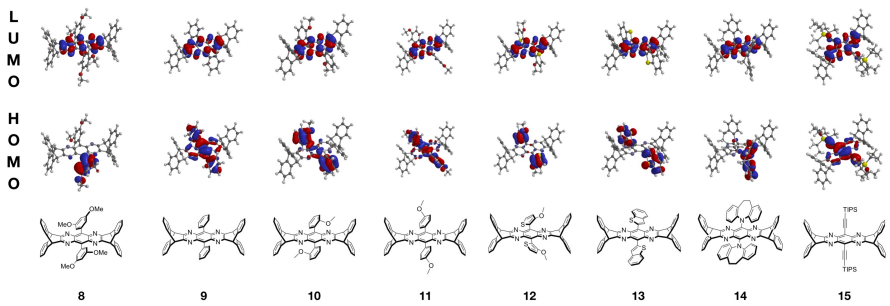

Figure 6: DFT calculations of HOMO and LUMO for compounds **8 – 15**. The calculations were performed using the B3LYP functional and 6-31+G* basis set.

We performed DFT calculations using the B3LYP functional and 6-31+G* basis set to evaluate the HOMO-LUMO separation of all of the products (Figure 6). They show, as anticipated, the iptycene wings do not contribute to either HOMO or LUMO states. The HOMO and LUMO frontier orbitals, however have sizable overlap in products **9**, **10** and **11**. The exchange energy that stabilizes the triplet is therefore significant and produces a larger ΔE_{ST} that decreases the coupling between the singlet and triplet states and reduces RISC. This is consistent with the experimental data that the aryl substituted products are TADF inactive. Our DFT calculations suggest that products **8**, **12** and **13** seem to have favorable spatial HOMO-LUMO separation that provides only minor orbital overlay and at the onset we expected these compounds to be TADF active. However, these are gas phase, ground state, calculations with equilibrium conformations. It is possible that in the excited state conformations and dynamics are present that promote larger ΔE_{ST} and competitive nonradiative relaxations. With regard to the latter, the quantum yields of these materials are modest to low. The TIPS-acetylene product **15** shows high overlap between the HOMO and LUMO states. This is inconsistent with TADF behavior. This effect may be the result of the silicon groups, however conformation of the origin of the intersystem crossing will require additional investigations that are beyond our initial synthetic studies that are the focus of this publication.

In conclusion, we report the synthesis of **7** through an optimized synthetic route. The in situ reduction of 4,7-dibromo-5,6-dinitrobenzo[*c*][1,2,5]thiadiazole was optimized to boost the yield to 72%. The versatility of the dibromoaryl intermediate **7** was exemplified in a variety of Suzuki-Miyaura cross-coupling reactions that proceed in moderate to excellent yields (65 – 99%), a Pd-catalyzed *N*-arylation with iminodibenzyl, and a Sonogashira reaction with (triisopropylsilyl)acetylene. Most of the products are luminescent with emission colors ranging from blue to orange. We anticipate this molecular scaffold could potentially be used to create new materials with useful electrooptical properties.

Acknowledgment

Financial support was provided through the Airforce Office of Scientific Research, a Cusanuswerk scholarship of ALS, a MITei fellowship of CCAV sponsored by Eni S.p.A., and the German Research Foundation (DFG) of JUE.

Supporting Information

Yes

Primary Data

No

References and Notes

(1) Krebs, F. C. *Sol. Energy Mater. Sol. Cells* **2009**, *93* (4), 394–412.
(2) Burgues-Ceballos, I.; Stella, M.; Lacharmoise, P.; Martinez-Ferrero, E. *J. Mater. Chem. A* **2014**, *2* (42), 17711–17722.
(3) Segal, M.; Baldo, M.; Holmes, R.; Forrest, S.; Soos, Z. *Phys. Rev. B* **2003**, *68* (7), 1–14.
(4) Adachi, C.; Baldo, M. A.; Thompson, M. E.; Forrest, S. R. *J. Appl. Phys.* **2001**, 90 (10), 5048–5051.
(5) Hashimoto, M.; Igawa, S.; Yashima, M.; Kawata, I.; Hoshino, M.; Osawa, M. *J. Am. Chem. Soc.* **2011**, 133 (27), 10348–10351.
(6) Baldo, M. A.; Adachi, C.; Forrest, S. R. *Phys. Rev. B - Condens. Matter Mater. Phys.* **2000**, 62 (16), 10967–10977.
(7) Peng, Q.; Obolda, A.; Zhang, M.; Li, F. *Angew. Chemie - Int. Ed.* **2015**, 54 (24), 7091–7095.
(8) Obolda, A.; Ai, X.; Zhang, M.; Li, F. *ACS Appl. Mater. Interfaces* **2016**, 8, 35472–35478.
(9) Uoyama, H.; Goushi, K.; Shizu, K.; Nomura, H.; Adachi, C. *Nature* **2012**, 492 (7428), 234–238.
(10) Luo, Y.; Aziz, H. *Adv. Funct. Mater.* **2010**, 20 (8), 1285–1293.
(11) Kondakov, D. Y.; Pawlik, T. D.; Hatwar, T. K.; Spindler, J. P. *J. Appl. Phys.* **2009**, 106 (12), 124510.
(12) Li, W.; Pan, Y.; Xiao, R.; Peng, Q.; Zhang, S.; Ma, D.; Li, F.; Shen, F.; Wang, Y.; Yang, B.; Ma, Y. *Adv. Funct. Mater.* **2014**, 24 (11), 1609–1614.
(13) Cui, L.-S.; Nomura, H.; Geng, Y.; Kim, J. U.; Nakanotani, H.; Adachi, C. *Angew. Chemie Int. Ed.* **2017**, 56, 1571–1575.
(14) Turro, N. J. Modern Molecular Photophysics; Benjamin Cummings, **1978**.
(15) Nakanotani, H.; Higuchi, T.; Furukawa, T.; Masui, K.; Morimoto, K.; Numata, M.; Tanaka, H.; Sagara, Y.; Yasuda, T.; Adachi, C. *Nat. Commun.* **2014**, 5, 4016.
(16) Goushi, K.; Yoshida, K.; Sato, K.; Adachi, C. *Nat. Photonics* **2012**, 6 (4), 253–258.
(17) Kawasumi, K.; Wu, T.; Zhu, T.; Chae, H. S.; Van Voorhis, T.; Baldo, M. A.; Swager, T. M. *J. Am. Chem. Soc.* **2015**, 137 (37), 11908–11911.
(18) Chavez III, R.; Cai, M.; Tlach, B.; Wheeler, D. L.; Kaudal, R.; Tsyrenova, A.; Tomlinson, A. L.; Shinar, R.; Shinar, J.; Jeffries-EL, M. *J. Mater. Chem. C* **2016**, *4* (17), 3765–3773.
(19) Lim, J.; Albright, T. A.; Martin, B. R.; Miljanić, O. S. *J. Org. Chem.* **2011**, *76* (24), 10207–10219.

Formatted: Font:7.5 pt

Deleted: 2017-05-062017-05-05

(20) Marsden, J. A; Miller, J. J.; Shirtcliff, L. D.; Haley, M. M. *J. Am. Chem. Soc.* **2005**, *127*, 2464–2476.
(21) Zucchero, A. J.; McGrier, P. L.; Bunz, U. H. F. *Acc. Chem. Res.* **2010**, *43*, 397–408.
(22) Kivala, M.; Diederich, F. *Acc. Chem. Res.* **2009**, *42*, 235–248.
(23) Endo, A.; Sato, K.; Yoshimura, K.; Kai, T.; Kawada, A.; Miyazaki, H.; Adachi, C. *Appl. Phys. Lett.* **2011**, 98 (8), 10–13.
(24) Hirata, S.; Sakai, Y.; Masui, K.; Tanaka, H.; Lee, S. Y.; Nomura, H.; Nakamura, N.; Yasumatsu, M.; Nakanotani, H.; Zhang, Q.; Shizu, K.; Miyazaki, H.; Adachi, C. *Nat. Mater.* **2015**, 14 (3), 330–336.
(25) Anthony, J. E. *Chem. Rev.* **2006**, 106 (12), 5028–5048.
(26) Li, J.; Zhang, Q. *ACS Appl. Mater. Interfaces* **2015**, 7 (51), 28049–28062.
(27) Swager, T. M. *Acc. Chem. Res.* **2008**, 41 (9), 1181–1189.
(28) Wright, M. W.; Welker, M. E. *J. Org. Chem.* **1996**, 61, 133–141.
(29) Zhang, L.; Jiang, K.; Li, G.; Zhang, Q.; Yang, L. *J. Mater. Chem. A* **2014**, 2, 14852–14857.
(30) Wang, E.; Hou, L.; Wang, Z.; Hellström, S.; Mammo, W.; Zhang, F.; Inganäs, O.; Andersson, M. R. *Org. Lett.* **2010**, 12 (20), 4470–4473.
(31) Huang, W.; Buchwald, S. L. *Chem. - A Eur. J.* **2016**, 22, 14186–14189.
(32) Ganschow, M.; Koser, S.; Hahn, S.; Rominger, F.; Freudenberg, J.; Bunz, U. H. F. *Chem. - A Eur. J.* **2017**, 23, 4415-4421.
(33) Tao, Y.; Yuan, K.; Chen, T.; Xu, P.; Li, H.; Chen, R.; Zheng, C.; Zhang, L.; Huang, W. *Adv. Mater.* **2014,** *26* (47), 7931-7958.
(34) Zhang, Q.; Li, J.; Shizu, K.; Huang, S.; Hirata, S.; Miyazaki, H.; Adachi, C. *J. Am. Chem. Soc.* **2012,** *134* (36), 14706-14709.

(35) Preparation of **2** and **3**
Following a literature procedure[21]

(36) Preparation of **7**
The optimized reaction was carried out in a 20 mL vial, containing zinc powder (470 mg, 7.19 mmol) suspended in AcOH (3.5 mL). Under stirring **5** (138 mg, 358 µmol) was added and the reaction mixture was heated to 60 °C for 1 h. The reduced colorless intermediate **6** was separated from the zinc powder by filtration through a pad of celite and added dropwise to a solution of **4** (61 mg, 260 µmol) in AcOH (1.5 mL) over 1 h. A yellow precipitate immediately formed. The solution was stirred for another 1 h and extracted several times with CH_2Cl_2 (20 mL) until the organic phase was colorless. The combined organic layers were washed with an aqueous $NaHCO_3$ solution (100 mL) and water (100mL). After evaporation of the solvent, the crude product was purified via column chromatography (SiO_2, hexane/CH_2Cl_2 3:1 → 0:1). The product (**7**, 65 mg, 93.8 µmol, 72%) was obtained as a yellow powder. ^{1}H-NMR (400 MHz, $CDCl_3$) δ [ppm] = 7.59 (dd, *J3* = 5.4 Hz, *J4* = 3.2 Hz, 4H, CH), 7.17 (dd, *J3* = 5.4 Hz, *J4* = 3.2 Hz, 4H, CH), 5.84 (s, 4H, CH).

(37) Preparation of compounds **8 – 13** (GP1)
A Schlenk flask was filled with **7** (10 mg, 14.4 µmol), arylboronic acid (2.2 equiv., 31.7 µmol) and K_3PO_4 (12.3 mg, 57.8 µmol), evacuated and purged with argon. A mixture of water/toluene/1,4-dioxane (1:1.8:5.5, 0.5 mL) was added and the resulting suspension degassed with argon for 15 min. Subsequently, $Pd_2(dba)_3$ (0.4 mg, 0.437 µmol) and P(*o*-tol)$_3$ (1.1 mg, 3.61 µmol) were added, and the reaction was heated to 60 °C for 14 h. Upon full conversion of the starting material, the reaction was diluted with CH_2Cl_2 (10 mL) and washed with water (15 mL) three times. The organic phase was dried over $MgSO_4$, the solvent evaporated under reduced pressure and the crude purified by column chromatography (SiO_2, gradient of hexane/ CH_2Cl_2).

(38) Preparation of **14**
In a heat gun dried Schlenk tube under an atmosphere of argon, a mixture of **7** (15 mg, 21.7 µmol), iminodibenzyl (9 mg, 47.7 µmol) and Pd-RuPhos-G4 (1.8 mg, 2.17 µmol) was dissolved in dry 1,4-dioxane (0.5 mL). The resulting mixture was degassed in a stream of argon for 10 min. At this point LiHMDS (0.1 M in THF, 54 µL, 54.2 µmol) was added. After heating to 60 °C for 16 h the reaction mixture was dissolved with CH_2Cl_2 and subsequently washed with water and brine. After drying over $MgSO_4$ and evaporating under reduced pressure, flash column chromatography (SiO_2, hexane/CH_2Cl_2 1:1) afforded the product as a yellow solid. ^{1}H NMR (500 MHz, CD_2Cl_2) δ [ppm] = 7.51 (dd, *J* = 5.4, 3.2 Hz, 8H), 7.14 (ddd, *J* = 8.6, 6.5, 2.4 Hz, 12H), 6.72 (td, *J* = 7.3, 1.2 Hz, 4H), 6.54 (ddd, *J* = 8.7, 7.2, 1.7 Hz, 4H), 6.37 (dd, *J* = 8.4, 1.2 Hz, 4H), 5.61 (s, 4H), 3.67 (s, 8H). HRMS (ESI) m/z: $[M + H]^+$: 921.3700; found 921.3703.

(39) Preparation of **15**
7 (20 mg, 28.9 µmol), $Pd(PPh_3)_4$ (6.4 mg, 5.54 µmol) and CuI (1.0 mg, 5.25 µmol) were suspended in THF/Et_3N (1:1, 1.5 ml). After degassing with argon for 15 min, TIPS-acetylene (150 µL, 578 µmol) was added and the resulting reaction mixture was stirred at 50 °C for 60 h. The green luminescent reaction mixture was quenched by addition of water (5 mL) and extracted three times with CH_2Cl_2 (10 mL). The combined organic layers were dried over $MgSO_4$ and the solvent was evaporated under reduced pressure. The crude was purified by column chromatography (SiO_2, hexane/CH_2Cl_2 4:1 to 1:2). **15** (15 mg, 57%) was obtained as a yellow solid. ^{1}H-NMR (400 MHz, $CDCl_3$) δ [ppm] = 7.54 (dd, *J3* = 5.4 Hz, J4 = 3.2 Hz, 8H, CH), 7.14 (dd, *J3* = 5.4 Hz, *J4* = 3.2 Hz, 8H, CH), 5.60 (s, 4H, CH), 1.34 (s, 36H, CH3), 1.26 (s, 6H, CH); ^{13}C-NMR (100 MHz, $CDCl_3$) δ [ppm] = 157.7, 141.7, 140.2, 127.0, 125.4, 121.3, 107.6, 55.4, 19.1, 11.9. HRMS (ESI) m/z: $[M + H]^+$: 895.4586; found 895.4566.

Deleted: <#>Preparation of **4** ... [1]

Deleted: ... [2]

Deleted: 2017-05-062017-05-05

Page 5: [1] Deleted **Constantin Voll** **5/6/17 5:34:00 PM**

Preparation of **4**

Under an argon atmosphere, DMSO (3.8 mL, 53.4 mmol) was dissolved in CH_2Cl_2 (215 mL) and cooled to -78 °C before TFAA (6.5 mL, 45.9 mmol) was added over 15 min. Then, a solution of diol **3** (3.6 g, 15.1 mmol) in CH_2Cl_2 (81 mL) and DMSO (40.5 mL) was added over 30 min. After stirring for 1 h at -78 °C, NEt_3 (14.6 mL, 105 mmol) was added and the reaction mixture slowly equilibrated to room temperature over 20 h. At this point, the reaction was quenched by the addition 2M hydrochloric acid (540 mL). The aqueous phase was extracted with CH_2Cl_2 (100 mL) eight times, the combined organic extracts washed with water and dried over $MgSO_4$. The solvent was subsequently evaporated and the residue purified by column chromatography (SiO_2, CH_2Cl_2). The product (**4**, 2.86 g, 12.2 mmol, 80%) was obtained as a yellow solid. ^{1}H-NMR (400 MHz, $CDCl_3$) δ [ppm] = 7.48 (dd, *J3* = 5.5 Hz, *J4* = 3.2 Hz, 4H, CH), 7.38 (dd, *J3* = 5.5 Hz, *J4* = 3.2 Hz, 4H, CH), 5.00 (s, 2H, CH).

Preparation of **5**[23]

Under stirring and cooled by ice, TFMS (26.0 mL, 294 mmol) was added dropwise to fuming nitric acid (3.4 mL, 81.5 mmol). Next, 4,7-dibromobenzo[*c*][1,2,5]thiadiazole (7.5 g, 25.5 mmol) was added in small portions over 20 min. The reaction mixture was stirred at 50 °C for 16 h, quenched by pouring on ice water and neutralized by addition of 4M NaOH (95 mL). The reaction mixture was filtered, the precipitate washed with water and recrystallized from ethanol (300 mL). The product **5** (5.25 g 13.6 mmol, 54%) was obtained as off-white crystals. Further product (920 mg, 2.4 mmol, 9%) was obtained as light brown crystals by evaporating the mother lye and recrystallizing the residue.

Page 5: [2] Deleted **Constantin Voll** **5/6/17 5:41:00 PM**

Preparation of **8**

According to GP1, **7** (10 mg) was coupled with 3,5- dimethoxybenzeneboronic acid (5.5 mg). The crude was purified by column chromatography (SiO_2, hexane/ CH_2Cl_2 2:1 → 0:1). The product (**11**, 11.6 mg, 14.4 µmol, 99%) was obtained as a yellow powder. ^{1}H-NMR (300 MHz, $CDCl_3$) δ [ppm] = 7.47 (dd, *J3* = 5.4 Hz, *J4* = 3.2Hz, 8H, CH),7.10 (dd, *J3*=5.4Hz, *J4* =3.2 Hz, 8H, CH),6.65 (t, *J*=2.3 Hz, 2H, CH), 6.62 (d, *J* = 2.3 Hz, 4H, CH), 5.58 (s, 4H, CH), 3.85 (s, 12H, CH3). HRMS (ESI) m/z: $[M + H]^+$: 807.2966; found 807.2954.

Preparation of **9**

According to GP1, **7** (10 mg) was coupled with phenylboronic acid (3.9 mg). The crude was purified by column chromatography (SiO_2, hexane/CH_2Cl_2 3:1 → 0:1). The product (**9**, 9.9 mg, 14.4 µmol, 99%) was obtained as a yellow powder. ^{1}H-NMR (300 MHz, $CDCl_3$) δ [ppm] = 7.59 – 7.58 (m, 2H) 7.57 (d, *J* = 1.8 Hz, 4H, CH), 7.51- 7.50(m, 4H), 7.47 (dd, *J3* =5.4Hz, J4 =3.2Hz, 8H, CH), 7.09 (dd, *J*3 =5.4Hz, *J4* =3.2Hz, 8H, CH), 5.54 (s, 4H, CH). HRMS (ESI) m/z: $[M + H]^+$: 687.2543; found 687.2539.

Preparation of **10**

According to GP1, **7** (10 mg) was coupled with 2- methoxybenzeneboronic acid (4.8 mg). The crude was purified by column chromatography (SiO_2, hexane/CH_2Cl_2 3:1 → 0:1). The product (**10**, 7.1 mg, 9.5 µmol, 66%) was obtained as a yellow powder. ^{1}H-NMR (300 MHz, CD_2Cl_2) δ [ppm] = 7.60 – 7.46 (m, 10H), 7.19 – 7.09 (m, 14H), 5.54 (s, 4H, CH), 3.54 (d, *J* = 13.5 Hz, 6H, CH) HRMS (ESI) m/z: $[M + H]^+$: 747.2755; found 747.2745.

Preparation of **11**

According to GP1, **7** (10 mg) was coupled with 4- methoxybenzeneboronic acid (4.8 mg). The crude was purified by column chromatography (SiO_2, hexane/CH_2Cl_2 2:1 → 0:1). The product (**12**, 10.7 mg, 14.4 µmol, 99%) was obtained as a yellow powder. ^{1}H-NMR (300 MHz, $CDCl_3$) δ [ppm] = 7.49 – 7.47 (m, 8H), 7.46 (d, *J* = 1.6 Hz, 4H, CH), 7.11 – 7.08 (m, 12H), 5.57 (s, 4H, CH), 4.00 (s, 6H, CH3). HRMS (ESI) m/z: $[M + H]^+$: 747.2755; found 747.2736.

Preparation of **12**

GP1 was carried out with **7** (10 mg) and 3-methoxythiophen-2- boronic acid pinacol ester (7.6 mg). The crude product was purified by column chromatography (SiO_2, hexane/CH_2Cl_2 2:1 → 0:1, including 10% NEt_3). The product (**14**, 7.5 mg, 9.9 µmol, 69%) was obtained as a yellow powder. HRMS (ESI) m/z: $[M + H]^+$: 759.1883; found 759.1900. ^{1}H NMR (500 MHz, CD_2Cl_2) δ [ppm] = 7.61 (m, 5H), 7.53 (9H, m), 7.14 (br, 13H), 5.63 (4H, br), 3.70, br). Due to low solubility, only a poor NMR spectrum could be obtained.

Preparation of **13**

According to GP1, **7** (10 mg) was coupled with thianaphthene-2- boronic acid (5.7 mg). The crude was purified by column chromatography (SiO_2, hexane/CH_2Cl_2 3:1 → 0:1). The product (**13**, 7.5 mg, 9.4 µmol, 65%) was obtained as an orange powder. Due to poor solubility, only a poor NMR spectrum could be obtained. HRMS (ESI) m/z: $[M + H]^+$: 799.1985; found 799.1967.